2026. Submitted Version DOI: 10.1111/jfd.70172
Journal of Fish Diseases, e70172.

Macroscopic examination of skeletal tissues in phosphorus-deficient rainbow trout *Oncorhynchus mykiss*

(Running title: Phosphorus-deficient skeletal changes)

Shozo H. Sugiura

Graduate School of Environmental Sciences. The University of Shiga Prefecture, Hikone-city, Shiga, Japan

Acknowledgements (Funding statement)

This work was supported in part by the institutional research fund of the University of Shiga Prefecture.

Data Availability Statement

The data that support the findings of this study are available from the corresponding author upon reasonable request.

Conflicts of Interest Statement

There are no conflicts of interest.

Ethics approval statement

The present study was conducted in accordance with the guidelines for animal experimentation established by the Bioresources Experiment Station, University of Shiga Prefecture (Approval code: 251042).

Abstract

Phosphorus (P) deficiency in aquacultured fish has become increasingly prevalent due to stricter environmental regulations and reduced dietary P inputs. The P status of fish is commonly assessed using P-gauge indicators such as bone P content, yet the skeletal regions most sensitive to P deficiency remain unclear. The present study examined various skeletal tissues in juvenile rainbow trout *Oncorhynchus mykiss* fed either a P-deficient or control diet for 1.5 months. Following formalin fixation, muscular tissues were enzymatically digested, and skeletons were stained with alizarin red, alcian blue, and aniline blue for detailed examination. P-deficient fish exhibited mild rib deformities and extensive non-calcified regions across the skeleton, fins, and scales, particularly at rib growth zones, neural and hemal arches, and in dentin. These findings were confirmed using scanning electron microscopy coupled with energy-dispersive X-ray spectroscopy (SEM-EDS). In contrast, heating P-deficient fish (70 or 100°C) to remove soft tissues markedly exacerbated skeletal deformities. The results indicate that expansion of non-calcified skeletal regions is a sensitive diagnostic indicator of P deficiency in farmed fish, and that heating low-P skeletons can artificially induce deformities that are not apparent in situ.

Keywords: phosphorus deficiency; fish rickets; systemic bone loss; skeletal deformities; bone decalcification; phosphorus deficiency indicators

Introduction

Rickets is a deficiency disease resulting from inadequate calcium (Ca), phosphorus (P), or vitamin D intake (Mughal, 2002; Wharton and Bishop, 2003; Chanchlani et al., 2020). The condition has been identified or experimentally induced in a variety of animal species. In aquacultured fish, rickets is primarily caused by P deficiency due to the reduced P content of formulated feeds, which is often legally regulated to minimize environmental pollution (Sugiura, 2018; Nathanailides et al., 2023; Flo et al., 2025).

As in higher vertebrates, P deficiency induces skeletal deformities in fish. Among these, hook-like deformities at the distal ends of ribs have been frequently reported by many researchers, including the present author (Murakami, 1967; Ogino et al., 1979; Shearer and Hardy, 1987; Baeverfjord et al., 1998; Vielma and Lall, 1998; Roberts et al., 2001; Sugiura et al., 2004).

However, in many of these studies, fish specimens were subjected to heating to facilitate the removal of adhering musculature prior to skeletal observation.

The non-calcified zone at the distal end of the ribs consists mainly of organic matrix composed of type I collagen (osteoid) and type II collagen (cartilage). Non-calcified collagens exhibit lower melting temperatures than their calcified counterparts (Kronick and Cooke, 1996; Yamashita et al. 2002; Bozec and Odlyha, 2011). Consequently, the characteristic curling of rib tips observed in some studies may not occur in vivo, but rather may be artifacts induced by heating during specimen preparation. To verify this possibility, a non-heating protocol must be applied and compared with conventional methods.

Among non-heating techniques, X-ray–based imaging is widely employed to detect skeletal abnormalities. However, non-calcified regions are difficult to visualize using X-rays due to their low contrast (e.g., Tepelenis et al., 2021; Meyer et al., 2023). Alizarin red specifically stains Ca and therefore labels only mineralized bone (cf. Materials and Methods). As a result, osteoid and other non-calcified tissues remain unstained. These can instead be counterstained with aniline blue or alcian blue, which selectively bind to collagen I and proteoglycans, respectively (Ralis and Watkins, 1992; Mouraret et al., 2014).

In the present study, this differential staining approach was employed to examine skeletal morphology in situ and to identify non-calcified regions. For comparison, the conventional heating method—where soft tissues are denatured by hot water and manually removed—was also performed.

Materials and Methods

Fish rearing and sampling conditions

Juvenile rainbow trout *Oncorhynchus mykiss* with an initial mean body weight of approximately 6 g (approximately 8 cm in total length) were obtained from a commercial trout farm. Fish were reared in 60 L plastic tanks supplied continuously with aerated freshwater from a well source (water temperature 16–18°C, pH 7.2-7.6, dissolved oxygen 9.0-11.0 ppm, P <0.01 ppm, Ca 6.4 ppm). Fish were hand-fed twice daily to apparent satiation for a period of 6 weeks. Comparisons of growth rate, feed efficiency, or other performance indices were not conducted because the feeding duration was relatively short and fish performance responses

to dietary P restriction have already been extensively studied. After the feeding period was completed, the fish were euthanized with an overdose of the anesthetic eugenol and subsequently either frozen or fixed in formalin for later analyses.

Ethics statement

The present study was conducted in accordance with the guidelines for animal experimentation established by the Bioresources Experiment Station, University of Shiga Prefecture (Approval code: 251042).

Diets

Fish were fed either a low-P diet (Table 1) or a commercial trout production feed (FEED ONE Co., Ltd., Yokohama, Japan). The low-P diet was prepared using washed ingredients to minimize inherent P content. The washed ingredients were mixed using a Hobart-type mixer with $FeCl_3$ dissolved in tap water and incubated overnight at room temperature. Subsequently, the remaining ingredients were added, and the resulting dough was cold-pelletized and air-dried at room temperature. The dried feed pellets were top-coated with a feed attractant to enhance palatability, and oils were added after drying. The total P content of the low-P diet was approximately 0.13%.

Skeletal examination (Staining protocol)

The general protocol followed previously published procedures (e.g., Dingerkus and Uhler, 1977; Taylor and Van Dyke, 1985; Gavaia et al., 2000; Depew, 2008; Aliesfehani, 2015) with minor modifications. Whole fish were fixed in 10% neutral buffered formalin for 10–20 days at room temperature. Specimens were then rinsed in running tap water for 24 h to remove residual formalin. Skin, eyes, gills, and internal organs were carefully removed prior to dehydration. Fish were sequentially dehydrated in 70% ethanol for 24 h and in 100% ethanol for an additional 24 h.

Specimens were then immersed for 1 h in dilute alcian blue solution (pH 2.5, Muto Pure Chemicals Co. Ltd., Tokyo, Japan) prepared in an ethanol:acetic acid mixture (4:1, v/v) to stain cartilage or type II collagen. The staining duration was minimized to prevent dissolution of osseous tissues (Gavaia et al., 2000). After staining, specimens were rinsed in tap water for 30 min. Muscular tissues were digested by incubating fish in 0.1 M phosphate buffer (pH 7.5) containing pancreatin (FUJIFILM Wako Pure Chemical Co., Osaka, Japan) at 35°C for

approximately 5 days. When the muscle tissue became translucent, the solution was replaced with 0.5% KOH containing alizarin red S (Merck Chemicals GmbH, Darmstadt, Germany) to stain mineralized bone. The staining duration ranged from 1 to 2 days. To facilitate further digestion of residual muscle, higher concentrations of KOH (1–3%) were occasionally used.

At each stage, photographs were taken either directly or under a stereomicroscope using various lighting conditions. To enhance the visibility of osteoid or type I collagen, aniline blue staining (pH2.4, Muto Pure Chemicals) was occasionally applied immediately before microscopic observation.

For scale examination, scales were collected from frozen–thawed specimens, then stained with alizarin red S (pH 6.5, phosphate buffer) for 3–20 min immediately before microscopic examination. Aniline blue was occasionally used to increase the visibility of external non-calcified regions.

During all soaking steps, plastic containers (7 × 11 × 2 cm) were continuously and gently agitated using a rotary mixer. P-deficient fish (n = 2) and control fish (n = 1) were always processed together in the same container to ensure identical experimental conditions. In total, 16 P-deficient fish and 8 control fish were examined and compared. Representative and high-clarity images were selected for examination and documentation.

Skeletal examination (Heating protocol)

Frozen whole fish were thawed prior to processing. Specimens were collectively heated for 5 min in hot water maintained at either 70 ± 1°C or 100 ± 1°C. The lower temperature (70°C) was selected as the minimum threshold required for protein denaturation in fish tissues (Schubring, 2009). Following heating, fish were immediately transferred to tap water for rapid cooling. When body temperature decreased to approximately 20°C, non-skeletal tissues, including muscles, viscera, skin, scales, and fins, were carefully removed using a gentle water jet. The isolated skeletons were reheated in hot water at the same temperatures as those used initially. The skeletons were then air-dried at room temperature and photographed.

For ash analysis, the spinal column of each dried skeleton was placed in a glass vial and defatted overnight in a chloroform:methanol mixture (1:1, v/v). The samples were then oven-dried at 105°C for 3 h to obtain dry weight and subsequently ashed at 550°C for 20 h to

determine ash weight. Based on previous reports, bone ash content was used as an indicator of Ca and P levels in the skeleton (Sugiura et al., 2004).

Elemental analysis

Three fish were randomly sampled from each of the low-P and control groups and stored at −20 °C until analysis. Frozen whole fish were thawed and heated collectively for 5 min in hot water (70 ± 1 °C). The dentary bones and caudal bones were then isolated, rinsed with tap water to remove adhering soft tissues, washed with acetone to remove lipids, and dried in a convection oven at 50 °C for 1 h. Scales were collected from frozen–thawed fish by scraping the dorsal region, rinsed with distilled water to remove adhering mucus, and air-dried at room temperature for 2–3 h.

The above samples were analyzed for elemental mass percentages (C, N, O, F, Na, Mg, Al, Si, P, S, Cl, K, Ca, Cr, Mn, Fe, Cu, Zn, Se, and Sr) using a scanning electron microscope (SEM; TM3030, Hitachi, Tokyo, Japan) equipped with an energy-dispersive X-ray spectrometer (EDS; AZtecOne, Oxford Instruments, UK). Scales were additionally analyzed for trace mineral contents (Mn, Fe, Cu, Zn, Sr, Cr, Se, Al, Mg, S, F, and Hg). Analyses were performed in low-vacuum mode at an accelerating voltage of 15 kV and a working distance of 8–10 mm.

Mean values (weight %) with standard deviations exceeding one-third of the mean (i.e., <3× signal-to-noise) were considered unreliable and were indicated accordingly. EDS quantification was normalized to 100% for the detected elements. Ratio analysis was also performed to normalize mineral contents relative to non-mineral elements such as O (oxygen) and S (sulfur), which exhibited relatively stable X-ray counts (low standard deviations). Stained samples were not used for elemental analysis because processing with acids and alkalis and dye binding may alter elemental composition.

Statistics

Elemental analyses were conducted in triplicate or more (n = 3–5 fish) for teeth and scales and in duplicate for caudal bones. Trace element analyses of scales were performed as single determinations for each of the low-P and control fish. Mean values were compared between low-P and control groups, as well as among specific tissue locations (e.g., enameloid vs. dentin), using Welch's t-test (assuming unequal variances) to detect significant differences.

The significance level was set at 5% ($p < 0.05$). Data are presented as mean ± SD (n), unless otherwise stated.

Results

The alcian blue–alizarin red–stained whole skeletons showed generally normal morphometry in both normal and low-P fish (Figure 1). Vertebral columns were largely straight in both groups; however, in low-P fish, individual vertebrae appeared more separated, and caudal bones exhibited weaker alizarin red staining compared to normal fish (Figure 2). The neural and hemal arches of low-P fish were not stained by alizarin red, in contrast to those of normal fish (Figures 3, 4). In low-P fish, the peripheral region of each vertebral body (vertebral ridge) also lacked alizarin red staining (Figure 4). The distal ends of the caudal skeleton displayed broader alizarin red–negative zones than those of normal fish (Figure 5).

The ribs of low-P fish were characterized by long alizarin red–negative stretches at their terminal ends, whereas ribs of control fish were well stained up to their growing ends (Figures 6, 7). Similarly, the growing ends of the neural and hemal spines in low-P fish exhibited non-calcified zones (photo not shown). Despite these differences in mineralization, their overall morphology was comparable to that of control fish.

Teeth of low-P fish contained alizarin red-negative dentin, unlike those of normal fish (Figures 8–10). The proximal end of the dentary also showed an alizarin red–negative region in low-P fish but not in normal fish (Figure 8). Heads and caudal fins of low-P fish showed weaker alizarin red staining than those of normal fish (Figures 11, 12). Scales of low-P fish exhibited alizarin red–negative peripheral zones that were not observed in control fish (Figure 13). Regenerating scales showed even broader alizarin red–negative areas than normal scales (photo not shown).

The heat-durability test showed that skeletal deformation upon heating occurred only in low-P fish and not in control fish (Figures 14–16). Among the low-P group, the severity of deformation was greater at the higher temperature (100°C) than at the lower temperature (70°C), and was more pronounced in fish with lower vertebral ash content than in those with higher ash content. Deformities in heated specimens—particularly in the ribs, neural and

hemal spines, and vertebral column (Figures 15, 16)—were evident when compared with stained, or non-heated specimens (Figures 1, 2).

Heating alizarin red and alcian blue–stained skeletons induced severe deformities even at 60°C for 3 min, particularly in the ribs and hemal–neural spines, in both low-P and control fish (photo not shown). This effect is presumably attributable to substantial decalcification resulting from the staining procedure.

SEM–EDS analysis provided independent evidence supporting the skeletal staining results. In control fish, Ca content was similar in dentin and enameloid (Table 2), and P content was also comparable between the two tissues. In both tissues, the P content (wt%) was approximately half that of Ca. In contrast, in low-P fish, both Ca and P contents in dentin were significantly lower than those in control fish ($p < 0.01$), in agreement with the EDS elemental mapping data (Figure 18). Ca and P contents in enameloid did not differ significantly between low-P and control fish.

In control fish, Mg and S contents were higher in dentin than in enameloid ($p < 0.01$). In low-P fish, Mg content was markedly reduced ($p < 0.01$) and S content was increased ($p < 0.05$) in dentin, but not in enameloid. Fluorine content tended to be higher in enameloid than in dentin in both control and low-P fish (data not shown due to high SD). Ca, P, and Mg contents in dentin normalized to O or S were also significantly lower in low-P fish than in control fish ($p < 0.01$).

EDS quantification did not allow reliable analysis of trace elements because their concentrations were much lower than those of major elements. In addition, light elements such as C and N were not accurately quantified under the present analytical conditions.

In scales, Ca and P contents were low in the marginal region of low-P fish but not in the central or off-center regions (Table 3), consistent with the EDS elemental mapping results (Figure 19). As observed in dentin, S content in the demineralized marginal region was higher than in the mineralized central and off-center regions. Ca and P contents normalized to O or S showed the same pattern, with reduced values in the scale margins. Scale Mg content was also lower in the marginal region than in the central or off-center regions (Table 4), and this trend remained after normalization to F or S. In contrast, Zn, S, and F contents in scales appeared to be stable regardless of dietary P status or scale region.

In control fish, Ca and P contents were higher in the proximal region of the caudal skeleton than in the more distal or marginal regions (Table 5). Mg content followed a similar trend, whereas S content showed the opposite pattern. In low-P fish, however, Ca, P, and Mg contents were uniformly low in both proximal and distal regions of the caudal skeleton, consistent with the EDS elemental mapping data (Figure 20). Normalization of Ca and P contents to O or S likewise indicated poor mineralization of the caudal skeleton in low-P fish.

Discussion

Systemic bone loss

Bones and scales serve as major reservoirs of P in fish. Consequently, P deficiency—whether resulting from inadequate dietary intake or physiological mobilization during gametogenesis—leads to significant bone mineral loss (e.g., Lopez et al., 1980; Kacem et al., 2000; Sbaihi et al., 2009; Sugiura, 2025a). In humans and other vertebrates, osteoid accumulation is a well-recognized feature of rickets (e.g., Mughal, 2002; Wharton and Bishop, 2003; Setiawati and Rahardjo, 2019; Chanchlani et al., 2020). Osteoid formation is typically more pronounced in endochondral bones such as vertebrae, ribs, and limb bones than in dermal bones such as the cranium, maxilla, and clavicle (Setiawati and Rahardjo, 2019; Demellawy et al., 2018).

The present study identified marked expansion of non-calcified regions in endochondral bones—including the growing ends of ribs, neural and hemal arches, the caudal skeleton, and the peripheral regions of the vertebral bodies—using alizarin red staining. However, comparable demineralized zones were also observed in dermal bones, such as the premaxilla, maxilla, dentary, operculum, as well as in fins and scales (Sire and Huysseune, 2003). These observations were generally consistent with the results obtained from SEM-EDS elemental analysis. Together, these findings indicate that P deficiency can induce systemic osteopenia, leading to widespread demineralization across diverse skeletal tissues.

Under P deficiency, P is mobilized from the skeleton to maintain essential soft-tissue metabolism (Kacem and Meunier, 2003; Aljuraibah et al., 2020; Serna and Bergwitz, 2020). As a result, skeletal tissues in P-deficient fish progressively become demineralized, leading to increases in (1) hypertrophic cartilage in endochondral bones, (2) newly formed or accumulated osteoid, and (3) demineralized (halastic) bone. These tissues may coexist within

decalcified or poorly mineralized regions. The present study, however, did not aim to differentiate these cell types or to elucidate their underlying molecular or physiological mechanisms. Several studies in fish have reported more detailed microscopic examination of non-calcified regions in bones or scales under dietary P deficiency (e.g., Roy et al., 2002; Witten et al., 2016, 2019; Cotti et al., 2020, 2024).

In the present study, Mg levels in dentin, caudal bones, and scales were reduced together with Ca and P (Table 5), suggesting that Mg is an essential component of hard tissues. This finding confirms earlier observations that P deficiency also decreases vertebral Mg content (e.g., Ogino and Takeda, 1978; Shearer and Hardy, 1987).

Ribs and neural-hemal spines

In rachitic infants, the anterior ends of the ribs—at the interface between the ribs and costal cartilage—develop a characteristic deformity known as the rachitic rosary or beading of the ribs. This lesion has long been recognized as one of the earliest and most sensitive clinical signs of rickets (Lawrence, 1880; Macewen, 1880; Hruska et al., 1996; Özkan, 2010; Akram et al., 2022). In contrast, such beading does not occur in fishes because their ribs are not articulated with costal cartilages (Kardong, 2006). Instead, as demonstrated in the present study, P deficiency in fish induces a conspicuous elongation of non-calcified zones at the growing ends of the ribs (Figures 6, 7).

In rachitic rosary lesions of mammals, the swelling at the costochondral junction is composed predominantly of unmineralized cartilage with relatively little osteoid (Sabbagh et al., 2005; Hoenerhoff and Brix, 2014; Walker et al., 2017). Histochemically, the non-calcified regions at the growing rib ends were faintly stained with alcian blue, a dye that binds strongly to proteoglycans and acidic mucopolysaccharides in cartilage (Scott and Dorling, 1965; Ippolito et al., 1983). Osteoid tissue also contains small amounts of proteoglycans, such as chondroitin sulfate, which allows weak binding of alcian blue and produces faint coloration. Thus, unfortunately, alcian blue labels both cartilage and, to a lesser extent, osteoid. In contrast, aniline blue selectively stains type I collagen in osteoid but does not react with cartilage (Mallory, 1936; Constantine and Mowry, 1968; Kiernan, 2015; Viola and Hindia, 2020).

In the present study, both dyes labeled non-mineralized (alizarin red–negative) areas, although aniline blue tended to produce more intense staining. To reliably discriminate between osteoid

and non-calcified cartilage, more precise control of staining parameters—such as pH, dye concentration, and staining and washing conditions—will be essential. Alternatively, more specific molecular approaches may be required.

Marked decalcification of the neural and hemal arches, as well as of the peripheral regions of each vertebra, is characteristic of low-P fish (Figures 2–4). This condition likely reduces mechanical strength and increases susceptibility to spinal deformities under handling stress. In addition, poorly mineralized collagen denatures at lower temperatures than well-calcified collagen, and therefore provides less protection against heat-induced damage (Kronick and Cooke, 1996; Yamashita et al., 2002). Consequently, P-deficient fish with poorly calcified bones could be more prone to developing skeletal deformities when reared at high temperatures, whereas they develop normally under cooler conditions. This situation is analogous to that of larval fish, whose bones are poorly calcified (McCay et al. 1936) and therefore more susceptible to deformities at elevated temperatures (Fraser et al., 2015).

Teeth and jawbones

Marked decalcification of dentin was evident in low-P fish compared with control fish (Figures 8–10). In contrast, the enameloid remained firmly mineralized under P-deficient conditions, as demonstrated by both alizarin red staining (Figures 8–10) and EDS elemental analysis (Figure 18; Table 2). These differences may reflect inherent differences in the degree of mineralization between dentin and enameloid. In mammals, enamel is highly mineralized, with approximately 96% (w/w) mineral content, consisting largely of hydroxyapatite, whereas dentin is substantially less mineralized (approximately 70%) (Teruel et al., 2015; Ortiz-Ruiz et al., 2018). Such differences may lead to distinct staining characteristics. Accordingly, in control fish, the enameloid region was poorly stained owing to its dense crystallization, whereas in low-P fish the same region appeared more intensely stained, possibly because reduced crystal density under P deficiency facilitated dye penetration.

However, this interpretation is not fully supported by the EDS data, as both Ca and P contents in the enameloid were similar between control and low-P fish. Since the penetration depth of the electron beam at an accelerating voltage of 15 kV is limited to only a few micrometers (Zohar et al., 2018; Martín et al., 2020; Zhang et al., 2023), Ca density in deeper layers may not have been captured by EDS.

In low-P fish, dentin decalcification was consistently detected by both alizarin staining and EDS analysis. This finding suggests that P deficiency may cause structural weakening of dentin and even tooth loss. Indeed, in the present study, many enameloid caps were lost during sample processing (e.g., washing and staining), particularly in low-P fish (Figure 10a). Earlier reports in humans and other animals are consistent with this observation (Fleischmann, 1878; Dick, 1916; Mellanby, 1918). Rickets and hypophosphatemia are now well established as causes of various dental abnormalities in humans, including enamel hypoplasia, dentin defects, and premature tooth loss (Schultz and Penner, 2023; Allam et al., 2025). The present findings suggest that fish rickets may share a similar etiology.

The pronounced decalcification observed at the base of the dentary (Figure 8a) further indicates that, under P-deficient conditions, not only the teeth but also the jaw bones are vulnerable to structural softening or deformation, consistent with previous reports of jaw-deformed fish (e.g., Roberts et al., 2001; Branson and Turnbull, 2008). In aquaculture, the risk of such dental and skeletal impairments is likely greatest during the early feeding stages, when dietary P requirements are highest relative to later life stages (e.g., Åsgård and Shearer, 1997; Sugiura, 2025b). Although such early defects may become evident only at later stages of development, by that time bone ash content (i.e., Ca and P levels) may have largely returned to normal, making it difficult to retrospectively identify dietary P deficiency as the underlying cause of deformity.

Caudal skeleton and caudal fin

In low-P fish, the caudal skeleton was only weakly stained by alizarin red compared with that of control fish (Figure 2), suggesting substantial decalcification, although faint red staining indicated the presence of small amounts of residual Ca. Nevertheless, SEM–EDS analysis, including both elemental mapping and point spectra, revealed little residual Ca or P in the caudal bones of low-P fish (Figure 20; Table 5). This discrepancy is likely attributable to analytical limitations of EDS, which probes only a very shallow surface layer, as discussed earlier.

Decalcification of the caudal fin was also evident in low-P fish (Figures 11, 12), suggesting that similar mineral loss may occur in other fins as well. In general, decalcified skeletal structures, including fin rays, are likely to exhibit reduced mechanical strength. Accordingly, fins of low-P fish may be more susceptible to erosion. Fin erosion is known to result from a wide range of

factors (e.g., Ellis et al., 2008; Klíma et al., 2013); however, P deficiency has not previously been recognized as a contributing cause. Given that aquacultured fish in recent years are increasingly fed low-P diets to comply with environmental regulations, such fish may have less mineralized fins and an increased risk of fin erosion. This possibility warrants further investigation.

Scales

Earlier studies have shown that scale ash, Ca, P, and Mg contents decrease substantially under dietary P deficiency, to levels even lower than those in bones (e.g., Davis and Robinson, 1987). Although the present study did not quantify these concentrations in scales, both alizarin red staining and EDS elemental analyses are consistent with these earlier reports.

The marginal region of scales was clearly decalcified under P-deficient conditions (Figures 13, 19, Table 3). From a practical standpoint, this finding is particularly noteworthy as a potential diagnostic indicator, because scales can be collected non-lethally, allowing the P status of many fish to be assessed simultaneously using simple alizarin red staining. This protocol is rapid, easy, and inexpensive, and therefore shows promise as an on-farm diagnostic tool.

However, further research is required to validate this approach, as P deficiency at fish farms is predominantly chronic (e.g., Deschamps et al., 2016). Most studies, including the present one, have focused on acute deficiency, which may differ substantially from chronic deficiency. Thus, the non-calcified regions observed here may be specific to acute P deficiency and may not be clearly detectable under chronic conditions. Further investigation of chronic P deficiency is therefore necessary before practical application.

Methodology for skeletal morphometry

P deficiency has been reported to cause skeletal deformities in various fish species. However, in most previous studies, bone morphology was assessed after removing soft tissues by heat denaturation. This procedure itself can induce artificial deformities, as poorly mineralized bones are less resistant to heat than normally calcified bones (e.g., Kronick and Cooke, 1996; Yamashita et al., 2002; Bozec and Odlyha, 2011). In addition, because the denaturation temperature of fish collagen—particularly in cold-water species—is substantially lower than that of homeothermic animals (Rigby, 1968; Jafari et al., 2020; Ahn et al., 2021; Farooq et al.,

2024), heat-based bone preparation may not be suitable for accurate bone morphometry, especially for poorly calcified bones of coldwater fishes, including rainbow trout.

The present results support this concern, as P-deficient fish exhibited only modest rib deformities in situ (Figures 1, 6, 7), whereas these deformities were markedly exaggerated after heating of the less-calcified ribs, manifesting as curling or hook-like bending at the growing tips (Figures 15, 16).

Therefore, when examining hypomineralized or rachitic bones, non-heating methods—such as X-ray, CT, MRI, or ultrasound imaging—are essential when preservation of native structural integrity is required. However, aside from X-ray analysis, these techniques are generally cost-prohibitive for diagnosing rickets or P deficiency in farmed fish. In the present study, a low-cost, non-heating staining method was employed. This method clearly differentiated calcified (red) from non-calcified (white or faint blue) regions across various bones, teeth, and scales, which could also serve as a practical diagnostic indicator of P deficiency in farmed fish.

Normal ribs are highly heat resistant, whereas ribs from P-deficient fish are heat labile. Because this difference manifests only upon heating, rib deformities are not apparent in situ in fresh fish but become evident after heat treatment. Therefore, assessment of rib deformity after heating remains a valid and useful diagnostic indicator for detecting incipient P deficiency in aquacultured fish.

Conclusions

P deficiency increased the extent of non-calcified regions across various osseous tissues, particularly at the growing ends of ribs and within the neural and hemal arches. Dental manifestations similar to those observed in mammals were also evident in P-deficient fish. Alizarin red staining of specific bones and scales may serve as a practical inexpensive diagnostic indicator of P deficiency in cultured fish. While P deficiency alone induced only mild skeletal deformities, exposure of the skeleton to elevated temperatures greatly intensified these deformities. As a future perspective, the effects of chronic P deficiency should be investigated, as this condition, rather than acute deficiency, is most relevant to commercial aquaculture production.

References

Ahn, H., Gong, D. J., Lee, H. H., Seo, J. Y., Song, K. M., Eom, S. J., & Yeo, S. Y. (2021). Mechanical properties of porcine and fish skin-based collagen and conjugated collagen fibers. Polymers, 13(13), 2151.

Akram, M., Anjum, A. A., Usman, M., Qaisar, I., & Malik, A. A. (2022). Rickets among children≤ 5 years of age presenting with poor growth visiting a tertiary healthcare facility. Professional Medical Journal, 29(08), 1203-1206.

Aliesfehani, T. (2015). Modified double skeletal staining protocols with Alizarinred and Alcian blue in laboratory animals. Annals of Military & Health Sciences Research, 13(2), 76-81.

Aljuraibah, F., Bacchetta, J., Brandi, M. L., Florenzano, P., Javaid, M. K., Mäkitie, O., ... & Wagner, C. A. (2020). An expert perspective on phosphate dysregulation with a focus on chronic hypophosphatemia. Journal of Bone and Mineral Research, 37(1), 12-20.

Allam, A., Cirio, S., Elia, F., Salerno, C., & Cagetti, M. G. (2025). Dental manifestations in children affected by hypophosphatemic rickets: A systematic review and meta-analysis. Children, 12(2), 144.

Åsgård, T., & Shearer, K. D. (1997). Dietary phosphorus requirement of juvenile Atlantic salmon, *Salmo salar* L. Aquaculture Nutrition, 3(1), 17-23.

Asin, J., Murphy, B. G., Samol, M. A., Polanco, J., Moore, J. D., & Uzal, F. A. (2021). Rickets in a Thoroughbred-cross foal: case report and review of the literature. Journal of Veterinary Diagnostic Investigation, 33(5), 987-992.

Baeverfjord, Åsgård, & Shearer. (1998). Development and detection of phosphorus deficiency in Atlantic salmon, *Salmo salar* L., parr and post-smolts. Aquaculture Nutrition, 4(1), 1-11.

Bozec, L., & Odlyha, M. (2011). Thermal denaturation studies of collagen by microthermal analysis and atomic force microscopy. Biophysical Journal, 101(1), 228-236.

Branson, E. J., & Turnbull, T. (2008). Welfare and deformities in fish. In: Fish Welfare (Branson, E.J., Ed.), Blackwell Publishing Ltd., Oxford, UK., pp. 202-216.

Chanchlani, R., Nemer, P., Sinha, R., Nemer, L., Krishnappa, V., Sochett, E., ... & Raina, R. (2020). An overview of rickets in children. Kidney International Reports, 5(7), 980-990.

Constantine, V. S., & Mowry, R. W. (1968). Selective staining of human dermal collagen: i. An analysis of standard methods. Journal of Investigative Dermatology, 50(5), 414-418.

Cotti, S., Di Biagio, C., Huysseune, A., Koppe, W., Forlino, A., & Witten, P. E. (2024). Matrix first, minerals later: fine-tuned dietary phosphate increases bone formation in zebrafish. JBMR plus, 8(8), ziae081.

Cotti, S., Huysseune, A., Koppe, W., Rücklin, M., Marone, F., Wölfel, E. M., ... & Witten, P. E. (2020). More bone with less minerals? The effects of dietary phosphorus on the post-cranial skeleton in zebrafish. International Journal of Molecular Sciences, 21(15), 5429.

Davis, D. A., & Robinson, E. H. (1987). Dietary phosphorus requirement of juvenile red drum Sciaenops ocellatus. Journal of the World Aquaculture Society, 18(3), 129-136.

Depew, M. J. (2008). Analysis of skeletal ontogenesis through differential staining of bone and cartilage. Molecular Embryology: Methods and Protocols, 37-45.

Deschamps, M. H., Poirier Stewart, N., Demanche, A., & Vandenberg, G. W. (2016). Preliminary study for description of bone tissue responsiveness to prolonged dietary phosphorus deficiency in rainbow trout, *Oncorhynchus mykiss* (Walbaum). Aquaculture Research, 47(3), 900-911.

Dick, J. L. (1916). The Teeth in Rickets. Proceedings of the Royal Society of Medicine, 9(Sect Study Dis Child), 83-91.

Dingerkus, G., & Uhler, L. D. (1977). Enzyme clearing of alcian blue stained whole small vertebrates for demonstration of cartilage. Stain Technology, 52(4), 229-232.

El Demellawy, D., Davila, J., Shaw, A., & Nasr, Y. (2018). Brief review on metabolic bone disease. Academic Forensic Pathology, 8(3), 611-640.

Ellis, T., Oidtmann, B., St-Hilaire, S., Turnbull, J. F., North, B. P., Macintyre, C. M., ... & Knowles, T. G. (2008). Fin erosion in farmed fish. In: Fish Welfare (Branson, E.J., Ed.), Blackwell Publishing Ltd., Oxford, UK. pp. 121-149.

Farooq, S., Ahmad, M. I., Zheng, S., Ali, U., Li, Y., Shixiu, C., & Zhang, H. (2024). A review on marine collagen: sources, extraction methods, colloids properties, and food applications. Collagen and Leather, 6(1), 11.

Fleischmann, L. (1878) Kieferrachitis. Dtsch. Vjschr. Zahnheilk. 18:180-185 (cited in: Seki, S., Tsuchida, S., Komoribayashi, N., Sekiyama, S., Nitanai, A. (1976) Oral manifestations of rickets. Dental Journal of Iwate Medical University 1(3): 143-149.

Flo, V. Ø., Åsgård, T., & Lekang, O. I. (2025). Phosphorus in salmonid aquaculture: sources, requirements, and system-level implications. Fishes, 10(8), 388.

Fraser, T. W. K., Hansen, T., Fleming, M. S., & Fjelldal, P. G. (2015). The prevalence of vertebral deformities is increased with higher egg incubation temperatures and triploidy in Atlantic salmon Salmo salar L. Journal of Fish Diseases, 38(1), 75-89.

Gavaia, P. J., Sarasquete, C., & Cancela, M. L. (2000). Detection of mineralized structures in early stages of development of marine Teleostei using a modified alcian blue-alizarin red double staining technique for bone and cartilage. Biotechnic & Histochemistry, 75(2), 79-84.

Hoenerhoff, M.J., Brix, A. (2014) Musculoskeletal system - Bone. In: Cesta MF, Herbert RA, Brix A, Malarkey DE, Sills RC (Eds.), National Toxicology Program Nonneoplastic Lesion Atlas. US Department of Health and Human Services.

Hruska, K. A., Slatopolsky, E., Schrier, R., & Gottschalk, C. (1996). Disorders of phosphorus, calcium, and magnesium metabolism. Disorders of the Kidney & Urinary Tract,, 3, 2295-2352.

Ippolito, E., Pedrini, V. A., & Pedrini-Mille, A. (1983). Histochemical properties of cartilage proteoglycans. Journal of Histochemistry & Cytochemistry, 31(1), 53-61.

Jafari, H., Lista, A., Siekapen, M. M., Ghaffari-Bohlouli, P., Nie, L., Alimoradi, H., & Shavandi, A. (2020). Fish collagen: extraction, characterization, and applications for biomaterials engineering. Polymers, 12(10), 2230.

Kacem, A., & Meunier, F. J. (2003). Halastatic demineralization in the vertebrae of Atlantic salmon, during their spawning migration. Journal of Fish Biology, 63(5), 1122-1130.

Kardong, K. V. (2006). Vertebrates: comparative anatomy, function, evolution (pp. 365-383). New York: McGraw-Hill.

Kiernan, J. (2015). Histological and histochemical methods. Scion publishing ltd.

Klíma, O., Kopp, R., Hadašová, L., & Mareš, J. (2013). Fin condition of fish kept in aquacultural systems. Acta Univ Agric Silvic Mendelianae Brun, 61(6), 1907-1916.

Kronick, P. L., & Cooke, P. (1996). Thermal stabilization of collagen fibers by calcification. Connective Tissue Research, 33(4), 275-282.

Lawrence, H. C. (1880). On infantile rickets. Lancet, 116(2979), 536-538.

Lopez, E., Mac Intyre, I., Martelly, E., Lallier, F., & Vidal, B. (1980). Paradoxical effect of 1.25 dihydroxycholecalciferol on osteoblastic and osteoclastic activity in the skeleton of the eel *Anguilla anguilla* L. Calcified Tissue International, 32(1), 83-87.

Macewen, W. (1880). Osteotomy with an inquiry into the aetiology and pathology of knock-knee, bow-leg, and other osseous deformities of the lower limbs. J. & A. Churchill, London.

Mallory, F. B. (1936). The anilin blue collagen stain. Stain Technology, 11(3), 101-102.

Martín, D., Moro, D., Ulian, G., & Valdrè, G. (2020). Monte Carlo SEM-EDS nano-microanalysis strategy of historical mineral pigments: the simulation of the Egyptian blue from pompeii (Italy) as an example. Minerals, 10(9), 807.

McCay CM, Tunison AV, Crowell M, Paul H (1936) The calcium and phosphorus content of the body of the brook trout in relation to age, growth, and food. J Biol Chem 114:259–263

Mellanby, M. (1918). An Experimental Study of the influence of diet on teeth formation. Lancet, 192(4971), 767-770.

Meyer, J., Rolvien, T., Reiter, A., Priemel, M., Frosch, K. H., Krukenberg, A., & Yarar-Schlickewei, S. (2023). Osteoid osteoma in the bones of the hand: a systematic literature review. Archives of Orthopaedic and Trauma Surgery, 143(8), 5437-5444.

Mouraret, S., Hunter, D. J., Bardet, C., Brunski, J. B., Bouchard, P., & Helms, J. A. (2014). A pre-clinical murine model of oral implant osseointegration. Bone, 58, 177-184.

Mughal, Z. (2002). Rickets in childhood. In Seminars in musculoskeletal radiology (Vol. 6, No. 3, pp. 183-190).

Murakami, Y. (1967) Studies on a cranial deformity in hatchery-reared young carp. Fish Pathology, 2(1): 1-10. (in Japanese)

Nathanailides, C., Kolygas, M., Tsoumani, M., Gouva, E., Mavraganis, T., & Karayanni, H. (2023). Addressing phosphorus waste in open flow freshwater fish farms: Challenges and solutions. Fishes, 8(9), 442.

Ogino, C., Takeda, H. (1978). Requirements of rainbow trout for dietary calcium and phosphorus. Bulletin of the Japanese Society of Scientific Fisheries, 44, 1019-1022.

Ogino, C., Takeuchi, L., Takeda, H., Watanabe, T. (1979) Availability of dietary phosphorus in carp and rainbow trout. Bull. Japan. Soc. Sci. Fish. 45 (12), 1527-1532.

Ortiz-Ruiz, A. J., de Dios Teruel-Fernández, J., Alcolea-Rubio, L. A., Hernández-Fernández, A., Martínez-Beneyto, Y., & Gispert-Guirado, F. (2018). Structural differences in enamel and dentin in human, bovine, porcine, and ovine teeth. Annals of Anatomy-Anatomischer Anzeiger, 218, 7-17.

Özkan, B. (2010). Nutritional Rickets. J Clin Res Ped Endo, 2(4), 137-143.

Ralis, Z. A., & Watkins, G. (1992). Modified tetrachrome method for osteoid and defectively mineralized bone in paraffin sections. Biotechnic & Histochemistry, 67(6), 339-345.

Rigby, B. J. (1968). Temperature relationships of poikilotherms and the melting temperature of molecular collagen. Biological Bulletin, 135(1), 223-229.

Roberts, R. J., Hardy, R. W., & Sugiura, S. H. (2001). Screamer disease in Atlantic salmon, *Salmo salar* L., in Chile. Journal of Fish Diseases, 24(9), 543-549.

Roy, P. K., Witten, P. E., Hall, B. K., & Lall, S. P. (2002). Effects of dietary phosphorus on bone growth and mineralisation of vertebrae in haddock (*Melanogrammus aeglefinus* L.). Fish Physiology and Biochemistry, 27(1), 35-48.

Sabbagh Y, Carpenter TO, Demay MB. (2005). Hypophosphatemia leads to rickets by impairing caspase-mediated apoptosis of hypertrophic chondrocytes. Proc Natl Acad Sci USA. 102:9637–9642. doi: 10.1073/pnas.0502249102.

Sbaihi, M., Rousseau, K., Baloche, S., Meunier, F., Fouchereau-Peron, M., & Dufour, S. (2009). Cortisol mobilizes mineral stores from vertebral skeleton in the European eel: an ancestral origin for glucocorticoid-induced osteoporosis?. Journal of Endocrinology, 201(2), 241.

Schubring, R. (2009). Differential scanning calorimetry. In: Fishery Products: Quality, safety and authenticity (Eds, Rehbein, H. and Oehlenschlager, J.). John Wiley & Sons, pp. 173-213.

Schultz, K. M., & Penner, C. R. (2023). A review of selected dental anomalies with histologic features in the pediatric patient. Pediatric and Developmental Pathology, 26(6), 572-582.

Scott, J. E., & Dorling, J. (1965). Differential staining of acid glycosaminoglycans (mucopolysaccharides) by alcian blue in salt solutions. Histochemie, 5(3), 221-233.

Serna, J., & Bergwitz, C. (2020). Importance of dietary phosphorus for bone metabolism and healthy aging. Nutrients, 12(10), 3001.

Setiawati, R., & Rahardjo, P. (2019). Bone development and growth. Osteogenesis and Bone Regeneration, 10, 82452.

Shearer, K. D., & Hardy, R. W. (1987). Phosphorus deficiency in rainbow trout fed a diet containing deboned fillet scrap. Progressive Fish-Culturist, 49(3), 192-197.

Sire, J. Y., & Huysseune, A. N. N. (2003). Formation of dermal skeletal and dental tissues in fish: a comparative and evolutionary approach. Biological Reviews, 78(2), 219-249.

Sugiura, S. H., Hardy, R. W., & Roberts, R. J. (2004). The pathology of phosphorus deficiency in fish–a review. Journal of Fish Diseases, 27(5), 255-265.

Sugiura, S. H. (2018). Phosphorus, aquaculture, and the environment. Reviews in Fisheries Science & Aquaculture, 26(4), 515-521.

Sugiura, S. H. (2025a). Evolutionary loss of acid-secreting stomach and endoskeletal ossification: A phosphorus perspective. Fishes, 10(2), 48.

Sugiura, S. H. (2025b). Nutrient requirements in diets: Fundamental issues in sustainable aquaculture development. Sustainability, 17(3), 1289.

Taylor, W., & Van Dyke, G. C. (1985). Revised procedures for staining and clearing small fishes and other vertebrates for bone and cartilage study. Cybium, 9(2), 107-119.

Tepelenis, K., Skandalakis, G. P., Papathanakos, G., Kefala, M. A., Kitsouli, A., Barbouti, A., ... & Kitsoulis, P. (2021). Osteoid osteoma: an updated review of epidemiology, pathogenesis, clinical presentation, radiological features, and treatment option. In Vivo, 35(4), 1929-1938.

Teruel J.D., Alcolea A., Hernández A., Ortiz A.J., 2015. Comparison of chemical composition of enamel and dentine in human, bovine, porcine and ovine teeth. Arch. Oral. Biol. 60, 768–775.

Vielma, J., & Lall, S. P. (1998). Control of phosphorus homeostasis of Atlantic salmon (*Salmo salar*) in fresh water. Fish Physiology and Biochemistry, 19(1), 83-93.

Viola, E., & Hindia, B. (2020). Connective tissue stains-a review. Int J Orofac Biol, 4, 4-9.

Walker, A., El Demellawy, D., & Davila, J. (2017). Rickets: historical, epidemiological, pathophysiological, and pathological perspectives. Academic Forensic Pathology, 7(2), 240-262.

Wharton, B., & Bishop, N. (2003). Rickets. Lancet, 362(9393), 1389-1400.

Witten, P. E., Fjelldal, P. G., Huysseune, A., McGurk, C., Obach, A., & Owen, M. A. (2019). Bone without minerals and its secondary mineralization in Atlantic salmon (*Salmo salar*): the recovery from phosphorus deficiency. Journal of Experimental Biology, 222(3), jeb188763.

Witten, P. E., Owen, M. A. G., Fontanillas, R., Soenens, M., McGurk, C., & Obach, A. (2016). A primary phosphorus-deficient skeletal phenotype in juvenile Atlantic salmon *Salmo salar*: the uncoupling of bone formation and mineralization. Journal of Fish Biology, 88(2), 690-708.

Yamashita, J., Li, X., Furman, B. R., Rawls, H. R., Wang, X., & Agrawal, C. M. (2002). Collagen and bone viscoelasticity: a dynamic mechanical analysis. Journal of Biomedical Materials Research, 63(1), 31-36.

Zhang, Y., Saravanakumar, K., & Çopuroğlu, O. (2023). Some critical reflections on the SEM-EDS microanalysis of the hydrotalcite-like phase in slag cement paste. Materials, 16(8), 3143.

Zohar, I., Massey, M. S., Ippolito, J. A., & Litaor, M. I. (2018). Phosphorus sorption characteristics in aluminum-based water treatment residuals reacted with dairy wastewater: 1. Isotherms, XRD, and SEM-EDS analysis. Journal of Environmental Quality, 47(3), 538-545.

Table 1. Ingredient composition of low-phosphorus feed

Ingredients	% (air-dry basis)
Soybean meal[1]	48
Blood meal[2]	10
Feather meal[3]	10
Wheat flour	7
CMC	2
Canola oil	10
Cod liver oil[4]	1
Vitamin premix[5]	2
Mineral premix[6]	8
Feed attractant[7]	2

[1] autoclaved at 120°C for 10 min, washed 2 times with 0.01N citric acid and 1 time with tap water.

[2] boiled in tap water, washed the curd 3 times with tap water.

[3] washed 1 time with 0.01N citric acid and 1 time with tap water.

[4] suppled vitamin A and D3 at approximately 12000IU and 1250IU/kg diet, respectively.

[5] supplied the following (mg/kg diet): thiamin hydrochloride 10; riboflavin 30; nicotinic acid 60; Ca pantothenate 50; pyridoxine hydrochloride 20; folic acid 10; d-biotin 1; vitamin B12 0.05; choline chloride 1500; myo-inositol 500; ascorbic acid 100; ascorbic acid 2 phosphate 50; alpha tocopherol acetate 1000; menadione Na bisulfite 30; BHT 100; L-lysine 5000 (filler dextrin). Vitamin E and BHT were added by dissolving in cod liver oil and canola oil.

[6] supplied the following: $CaCO_3$ 5%; NaCl 1%; KCl 1%; $FeCl_3$ 1%; other minerals (mg/kg diet as solution): $MgSO_4 \cdot 7H_2O$ 7500; $ZnSO_4 \cdot 7H_2O$ 500; $MnSO_4 \cdot 5H_2O$ 200; $CuSO_4 \cdot 5H_2O$ 30; KI 3; Na_2SeO_3 2; $CoCl_2 \cdot 6H_2O$ 2.

[7] autolyzed krill paste (NaCl 24%). Top dressed on dried feed pellets.

Table 2. Composition of selected minerals in the teeth of rainbow trout fed normal- or low-phosphorus diets

Element	Normal fish		Low-P fish		*p* value			
	Dentin	Enameloid	Dentin	Enameloid	normal dentin vs. normal enameloid	low-P dentin vs. low-P enameloid	normal dentin vs. low-P dentin	normal enameloid vs. low-P enameloid
	Wt% (mean ± SD)							
O	36.0 ± 6.65	47.1 ± 8.02	36.4 ± 0.96	36.4 ± 4.27	0.03	0.99	0.88	0.03
Mg	0.88 ± 0.17	*0.14 ± 0.13	*0.10 ± 0.05	0.42 ± 0.18	0.00	0.03	0.00	0.05
P	12.99 ± 1.90	12.30 ± 1.35	1.03 ± 0.58	12.68 ± 0.64	0.48	0.00	0.00	0.57
S	0.33 ± 0.07	*0.07 ± 0.02	2.09 ± 0.87	0.21 ± 0.14	0.00	0.02	0.03	0.14
Ca	24.92 ± 4.18	24.42 ± 4.85	1.00 ± 0.79	27.42 ± 2.46	0.85	0.00	0.00	0.24
Na	*0.28 ± 0.17	0.71 ± 0.18	*0.18 ± 0.09	0.56 ± 0.19	0.00	0.02	0.27	0.28
K	0.24 ± 0.10	0.22 ± 0.08	*0.17 ± 0.04	0.20 ± 0.05	0.67	0.41	0.19	0.73
	Ratio (mean ± SD)							
Ca/P	1.91 ± 0.05	1.97 ± 0.20	0.86 ± 0.30	2.16 ± 0.17	0.51	0.00	0.00	0.14
Ca/O	0.71 ± 0.17	0.55 ± 0.24	0.03 ± 0.02	0.76 ± 0.14	0.22	0.00	0.00	0.11
Ca/S	80 ± 22	*413 ± 163	0.43 ± 0.22	199 ± 137	0.00	0.06	0.00	0.05
P/O	0.37 ± 0.08	0.27 ± 0.09	0.03 ± 0.02	0.35 ± 0.04	0.07	0.00	0.00	0.08
P/S	41.8 ± 11.2	*211.0 ± 88.0	0.47 ± 0.16	91.6 ± 62.6	0.00	0.06	0.00	0.03
Mg/O	0.02 ± 0.01	*0.00 ± 0.00	*0.00 ± 0.00	0.01 ± 0.00	0.00	0.01	0.00	0.02
Mg/S	2.88 ± 0.96	*2.22 ± 2.21	*0.05 ± 0.02	2.96 ± 2.62	0.52	0.11	0.00	0.66

Each value represents the mean of 4–6 EDS determinations of elemental weight percentage (Wt%). SD: standard deviation (*n* = 4–6).

Values marked with asterisks should be regarded as semi-quantitative because of the high standard deviations indicated by the AZtecOne quantification algorithm.

Co-analyzed elements (C, N, Al, Si, Mn, Fe, Cu, Zn, Sr, Cl, F, Cr, and Se) were below the quantification limit because of low concentrations and/or high standard deviations.

Table 3. Composition of selected minerals in the scale of rainbow trout fed normal- or low-phosphorus diets

Element	Normal fish		Low-P fish							
	whole		whole		center		off-center		margin	
	Wt% (mean ± SD)									
C	44.5	± 6.5	43.9	± 7.4	*6.32	± 9.92	*12.9	± 8.56	46.0	± 11.1
O	38.2	± 5.7	42.4	± 7.3	47.1	± 5.0	44.9	± 4.5	37.3	± 7.3
Si	*0.12	± 0.08	0.41	± 0.14	0.37	± 0.09	0.31	± 0.08	*0.20	± 0.13
P	6.20	± 0.95	4.85	± 0.89	13.87	± 1.50	12.39	± 1.25	2.35	± 0.57
S	0.20	± 0.08	0.88	± 0.19	0.47	± 0.09	0.55	± 0.09	1.86	± 0.41
Ca	12.59	± 1.93	9.74	± 1.77	27.56	± 2.98	24.21	± 2.43	5.82	± 1.51
	Ratio (mean)									
Ca/P	2.03		2.02		1.98		1.95		2.29	
Ca/O	0.33		0.23		0.59		0.54		0.18	
Ca/S	84.9		10.9		59.7		44.0		3.2	
P/O	0.16		0.11		0.29		0.28		0.07	
P/S	41.9		5.4		29.9		22.5		1.2	

Each value represents the mean of duplicate or triplicate determinations of elemental weight percentage (Wt%), with the SD estimated by the AZtecOne quantification algorithm.

Values marked with asterisks should be regarded as semi-quantitative because of the high standard deviations indicated by the AZtecOne algorithm.

Co-analyzed elements (N, Mg, Al, Mn, Fe, Cu, Zn, Sr, Na, K, Cl, F, Cr, and Se) were below the quantification limit because of low concentrations and/or high standard deviations.

Table 4. Composition of specific minerals in the scale of rainbow trout fed normal- or low-phosphorus diets

Element	Normal fish	Low-P fish			
	whole	whole	center	off-center	margin
		Wt% (mean ± SD)			
Zn	11.66 ± 1.72	9.17 ± 2.32	10.89 ± 3.44	10.28 ± 2.65	11.93 ± 3.26
Mg	10.03 ± 0.85	5.46 ± 0.99	10.30 ± 1.69	8.07 ± 1.24	*0.03 ± 1.39
S	9.4 ± 0.59	10.3 ± 0.79	10.6 ± 1.20	15.7 ± 1.21	14.3 ± 1.38
F	61.3 ± 2.40	65.2 ± 3.28	57.9 ± 4.17	54.4 ± 3.26	64.4 ± 4.96
		Ratio (mean)			
Mg/F	0.16	0.08	0.18	0.15	*0.00
Mg/S	1.07	0.53	0.97	0.51	*0.00

Each value represents a single EDS determination of elemental weight percentage (Wt%) with the SD estimated by the AZtecOne quantification algorithm.

Values marked with asterisks should be regarded as semi-quantitative because of the high standard deviations indicated by the AZtecOne algorithm.

Co-analyzed elements (Mn, Fe, Cu, Sr, Cr, Se, Al, and Hg) were below the quantification limit because of low concentrations and/or high standard deviations.

Table 5. Composition of selected minerals in the caudal skeleton of rainbow trout fed normal- or low-phosphorus diets

Element	Normal fish			Low-P fish		
	whole	center	margin	whole	center	margin
	Wt% (mean ± SD)					
C	33.5 ± 5.1	*11.6 ± 15.8	*36.5 ± 14.4	47.8 ± 5.8	38.6 ± 5.4	42.4 ± 8.9
O	36.4 ± 3.0	37.9 ± 7.4	42.0 ± 10.3	42.4 ± 4.8	40.8 ± 4.0	39.1 ± 6.5
Mg	0.74 ± 0.08	1.55 ± 0.34	*0.17 ± 0.16	*0.02 ± 0.08	*0.07 ± 0.09	*0.00 ± 0.13
P	8.19 ± 0.68	14.78 ± 2.86	3.89 ± 0.97	0.95 ± 0.13	0.67 ± 0.10	0.71 ± 0.18
S	0.58 ± 0.06	*0.30 ± 0.12	3.15 ± 0.80	1.84 ± 0.22	1.60 ± 0.18	3.90 ± 0.66
Ca	14.81 ± 1.23	25.36 ± 4.91	5.32 ± 1.33	0.34 ± 0.08	0.44 ± 0.09	0.69 ± 0.20
K	0.28 ± 0.04	*0.40 ± 0.14	1.89 ± 0.51	0.54 ± 0.09	0.30 ± 0.08	1.87 ± 0.35
	Ratio (mean)					
Ca/P	1.81	1.72	1.37	0.36	0.66	0.97
Ca/O	0.41	0.67	0.13	0.01	0.01	0.02
Ca/S	25.5	*84.5	1.7	0.2	0.3	0.2
P/O	0.23	0.39	0.09	0.02	0.02	0.02
P/S	14.1	*49.3	1.2	0.5	0.4	0.2

Each value represents a single EDS determination of elemental weight percentage (Wt%), with the SD estimated by the AZtecOne quantification algorithm.

Values marked with asterisks should be regarded as semi-quantitative because of the high standard deviations indicated by the AZtecOne algorithm.

Co-analyzed elements (N, Al, Mn, Fe, Cu, Zn, Sr, Na, K, Cl, F, Cr, and Se) were below the quantification limit because of low concentrations and/or high standard deviations.

Figure legends

Figure 1. Whole skeletons of a normal fish (top) and a low-P fish (bottom) stained simultaneously in the same tray with alcian blue and alizarin red. Residual soft tissues (white) remain adherent to the hard tissues. In the low-P fish, the growing ends (tips) of the ribs are stained blue (arrows). In both normal and low-P fish, no apparent deformities are observed in the hemal and neural spines or in the ribs. Scale bar = 2 cm.

Figure 2. Vertebral columns of low-P fish (top two) and a normal fish (bottom) stained simultaneously in the same tray with alizarin red. In the low-P fish, individual vertebrae are more distinctly separated (red arrows), and the caudal skeleton shows weaker staining (black arrows) compared with the normal fish. Scale bar = 2 cm.

Figure 3. Vertebral columns of a low-P fish (top) and a normal fish (bottom). White, non-calcified areas are evident in the neural and hemal arches of the low-P fish (black and yellow arrows). Scale bar = 2 mm.

Figure 4. (a) Vertebrae of a low-P fish (left) and a normal fish (right). Non-calcified areas are visible in the neural and hemal prezygapophyses and postzygapophyses (arrows). (b) Vertebrae of a low-P fish (left) and a normal fish (right), showing non-calcified areas in the neural and hemal arches (arrows). The white periphery of the vertebral body (arrow) also indicates a distinct non-calcified zone compared to the normal fish. Scale bar = 1 mm.

Figure 5. Caudal skeletons of a low-P fish (left) and a normal fish (right). Note the increased non-calcified zones in the hypural and parhypural regions of the low-P fish (arrows). Scale bar= 1 mm.

Figure 6. Growing ends of ribs stained in situ. (a) Low-P fish; (b) normal fish. Non-calcified regions at the rib tips are stained blue and largely straight (arrows). R: pleural rib; M: intercostal muscle. Scale bar = 1 mm.

Figure 7. Pleural ribs of a low-P fish (a) and a normal fish (b). Insets show higher-magnification views. Extended non-calcified regions are present in the ribs of the low-P fish (arrows). The calcified portion of the low-P rib appears slightly deformed or kinked. Scale bar = 2 mm.

Figure 8. Dentaries of a low-P fish (a) and a normal fish (b) stained with alizarin red. In the low-P fish, non-calcified dentin (black arrow) is visible beneath the calcified enameloid cap (red arrow). Note also the distinct non-calcified area at the base of the dentary (triangle). Scale bar = 1 mm.

Figure 9. Premaxillary (P) and maxillary (M) bones of a low-P fish. Note the white, non-calcified dentin (arrow). Scale bar = 2 mm.

Figure 10. (a) Premaxillae of a normal fish (left) and a low-P fish (right). The low-P fish shows a white non-calcified zone along the periphery (white arrow). Enameloid caps are lost in the low-P fish (black arrow), either in vivo or during analysis. (b) Teeth of a normal fish (left) and a low-P fish (right). Enameloid caps of the normal fish are only weakly stained (arrow). Scale bar = 1 mm.

Figure 11. Head and tail regions of low-P fish (top two) and a normal fish (bottom) stained simultaneously in the same tray with alizarin red. The head of the low-P fish shows weaker staining intensity than that of the normal fish. The terminal region of the caudal fin of the low-P fish is unstained (arrows), whereas the same region of the normal fish is stained red (arrow). Scale bar = 1 cm.

Figure 12. Terminal regions of the caudal fins of a low-P fish (top) and a normal fish (bottom), stained simultaneously in the same tray with alizarin red and counterstained with aniline blue. The terminal region of the caudal fin in the low-P fish is less calcified (arrow). Scale bar = 5 mm.

Figure 13. Scales of low-P fish (a) and normal fish (b). Distinct unstained peripheral zones (arrows) are evident in the low-P fish, whereas these regions are nearly absent in the normal fish. Scale bar = 200 µm.

Figure 14. Vertebral columns of low-P (Low-P) and normal (Norm) fish heated at either 70°C for 5 min or 100°C for 5 min. Numbers indicate body weight (g) and vertebral ash content (%). No deformities were observed in normal fish at either temperature. Low-P fish exhibited vertebral deformities, which were more pronounced at 100°C than at 70°C (Figures 15-16). Scale bar = 5 cm.

Figure 15. (Magnified from Figure 14) Vertebral columns of low-P fish #1–5 (from top to bottom) heated simultaneously in the same bath at 70°C for 5 min. Numbers indicate body

weight (g) and vertebral ash content (%). Note wavy ribs and neural–hemal spines (arrows). Scale bar = 1 cm.

Figure 16. (Magnified from Figure 14) Vertebral columns of low-P fish #1–5 (from top to bottom) heated simultaneously in the same bath at 100°C for 5 min. Numbers indicate body weight (g) and vertebral ash content (%). Note wavy ribs, neural–hemal spines, and vertebral columns (arrows). Scale bar = 1 cm.

Figure 17. Examples of analytical regions in teeth (A: top, dentin; bottom, enameloid), scales (B: from top to bottom, margin, off-center, and center), and caudal bones (C: left, center; right, margin), indicated by yellow arrows. Corresponding analytical data are summarized in Tables 2–5.

Figure 18. EDS elemental mapping of calcium (blue) and phosphorus (red) in teeth. (A) Normal fish, showing Ca and P signals in both dentin and enameloid regions. (B) Low-P fish, in which Ca and P signals are detected only in the enameloid region at the tooth tip (white arrows).

Figure 19. EDS elemental mapping of calcium (blue) and phosphorus (red) in a scale from a low-P fish. The white dotted line indicates the boundary of the scale. Another scale partially overlaps the lower-left corner. Note that Ca and P signals are detected only in the central region. In scales from normal fish, Ca and P signals are present throughout the entire scale (figure not shown).

Figure 20. EDS elemental mapping of calcium (blue) and phosphorus (red) in the caudal skeleton (hypurals and parhypural) of a low-P fish (left) and a normal fish (right), analyzed simultaneously within the same field of view. Note the marked difference in Ca and P signal intensities between low-P and normal fish. White dotted lines indicate the boundaries of the caudal bones.

Figure 1.

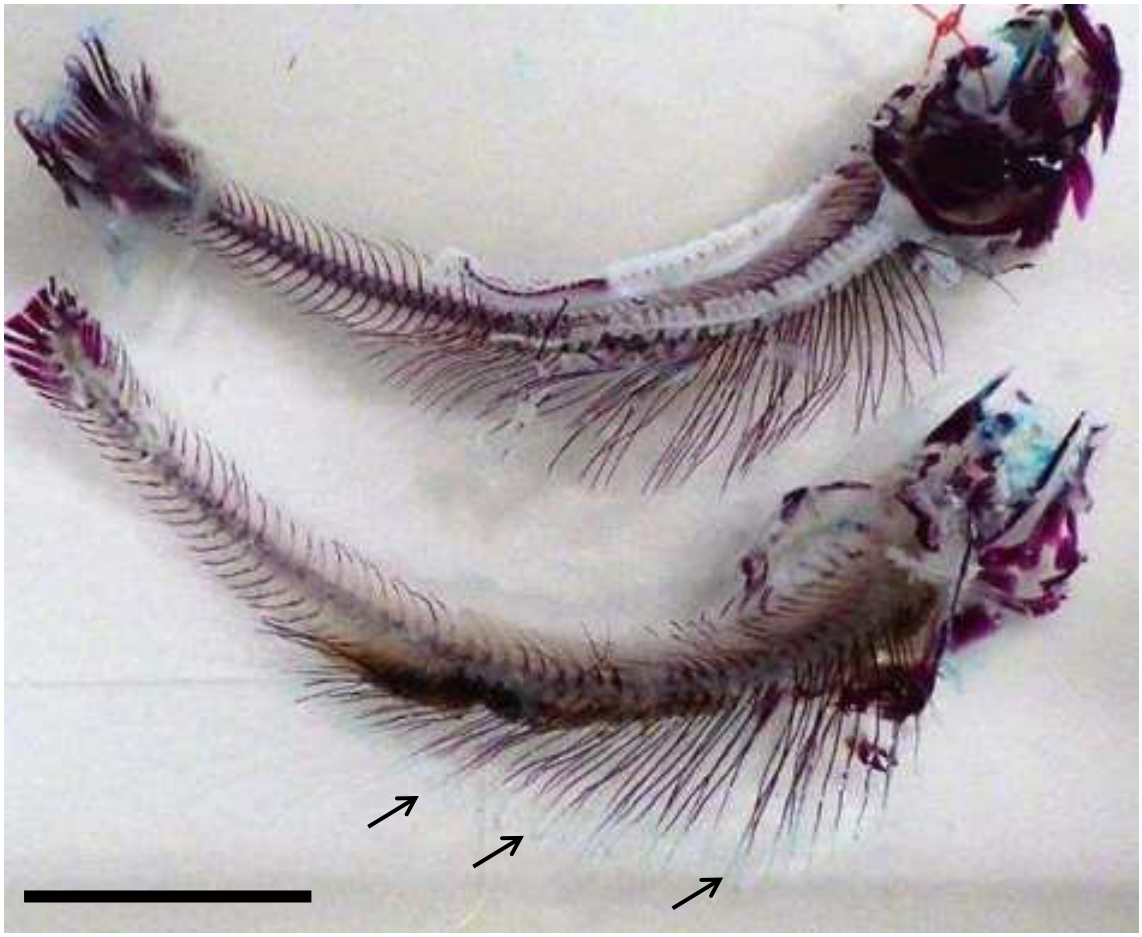

Figure 2.

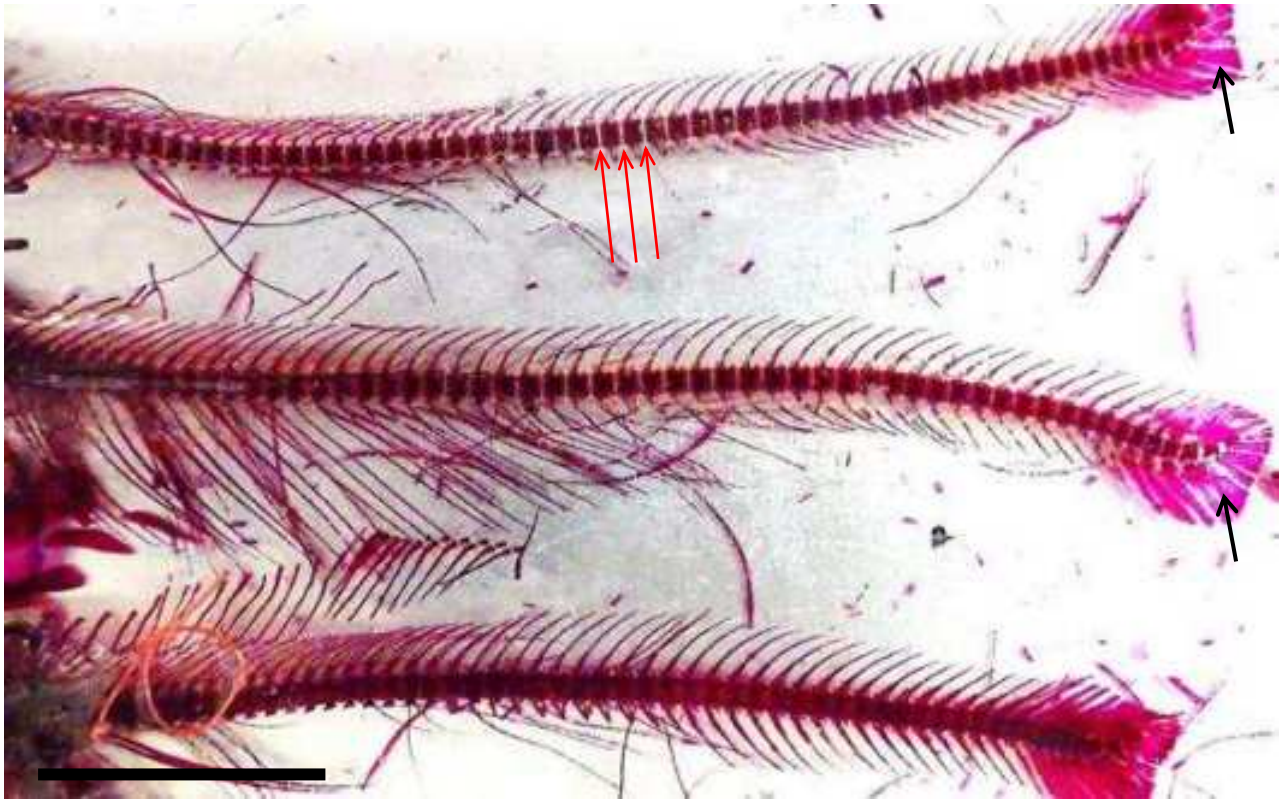

Figure 3.

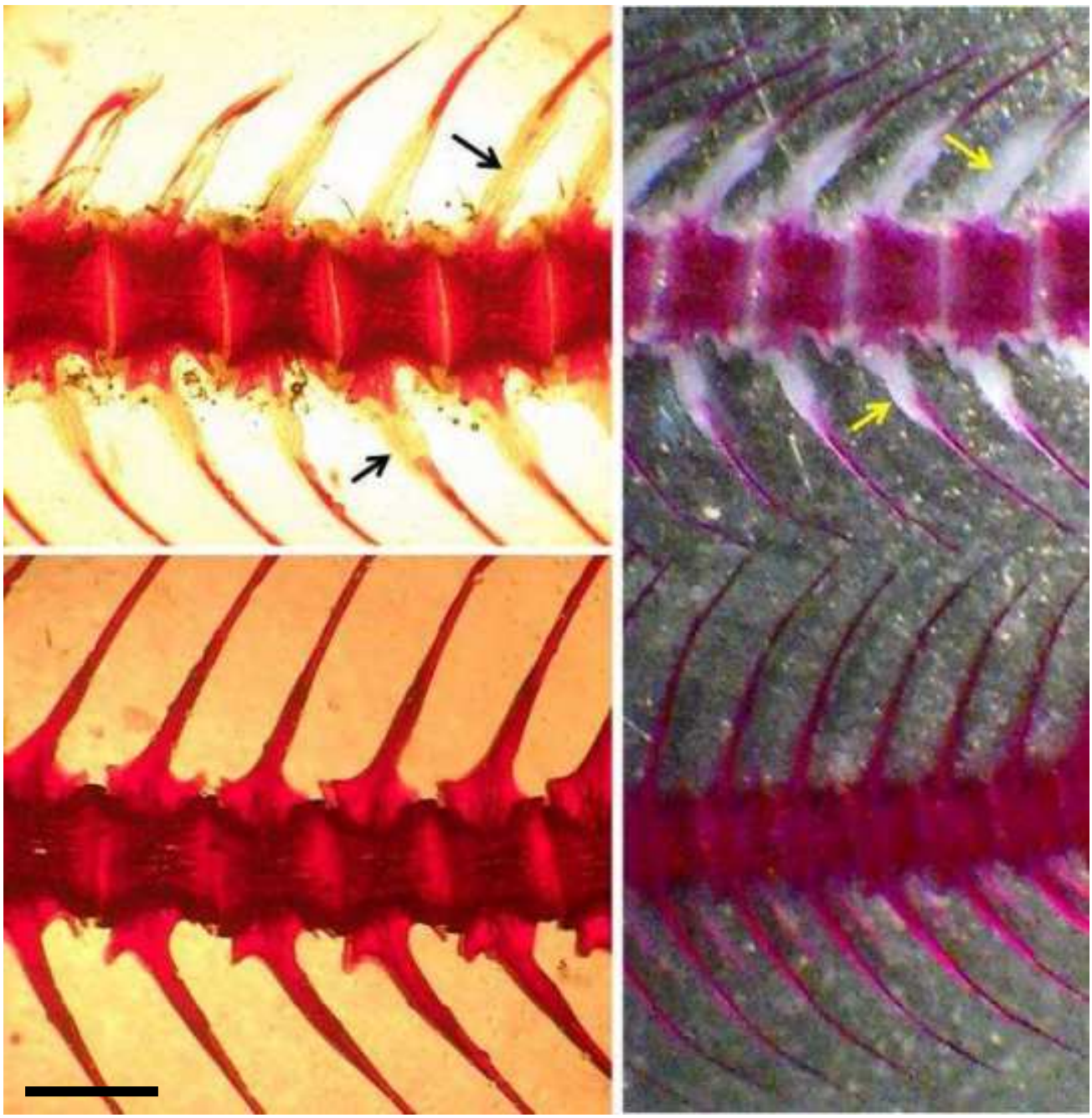

Figure 4.

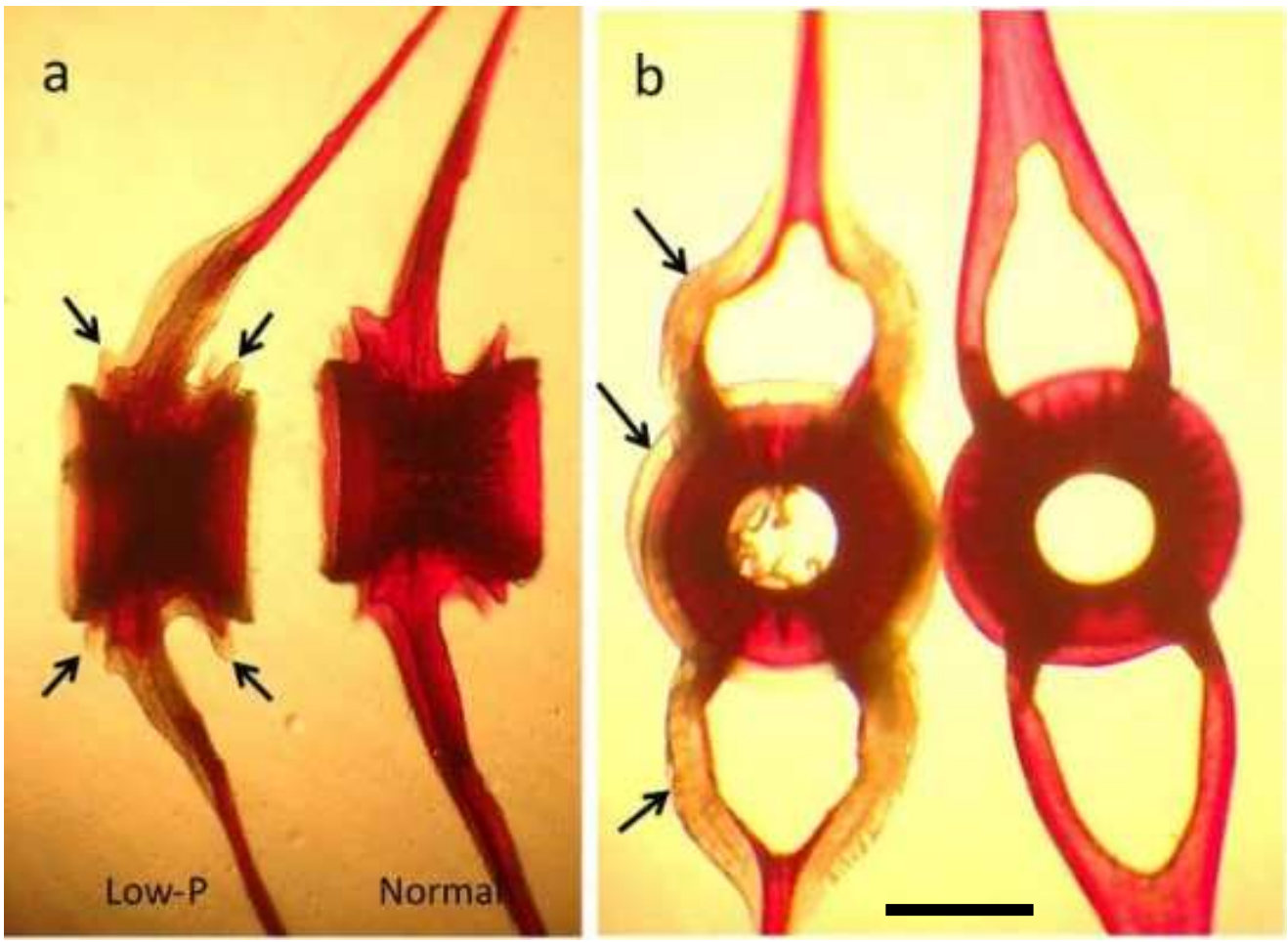

Figure 5.

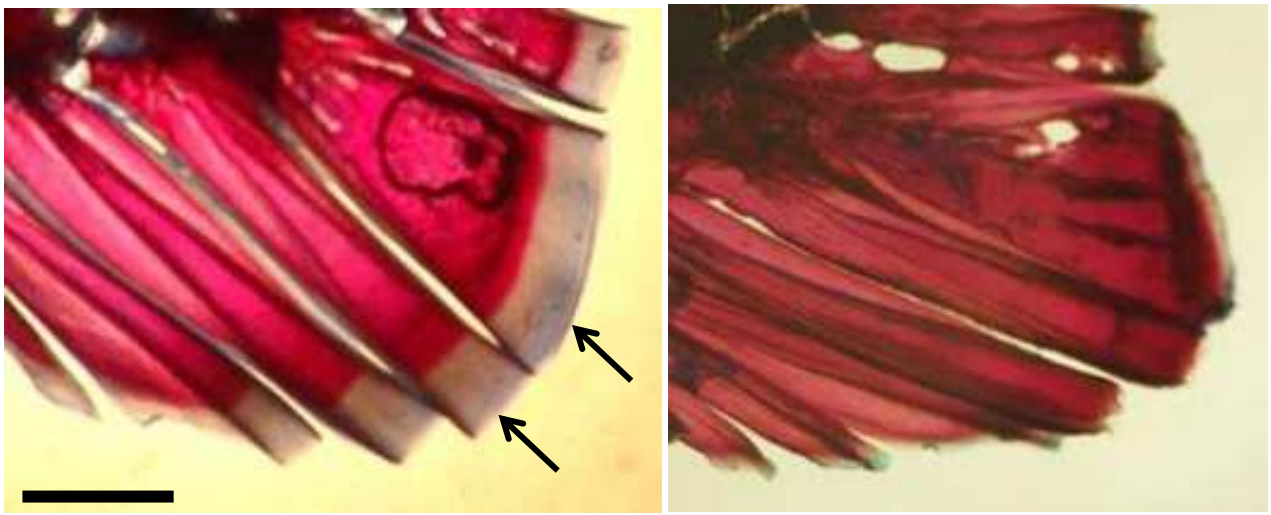

Figure 6.

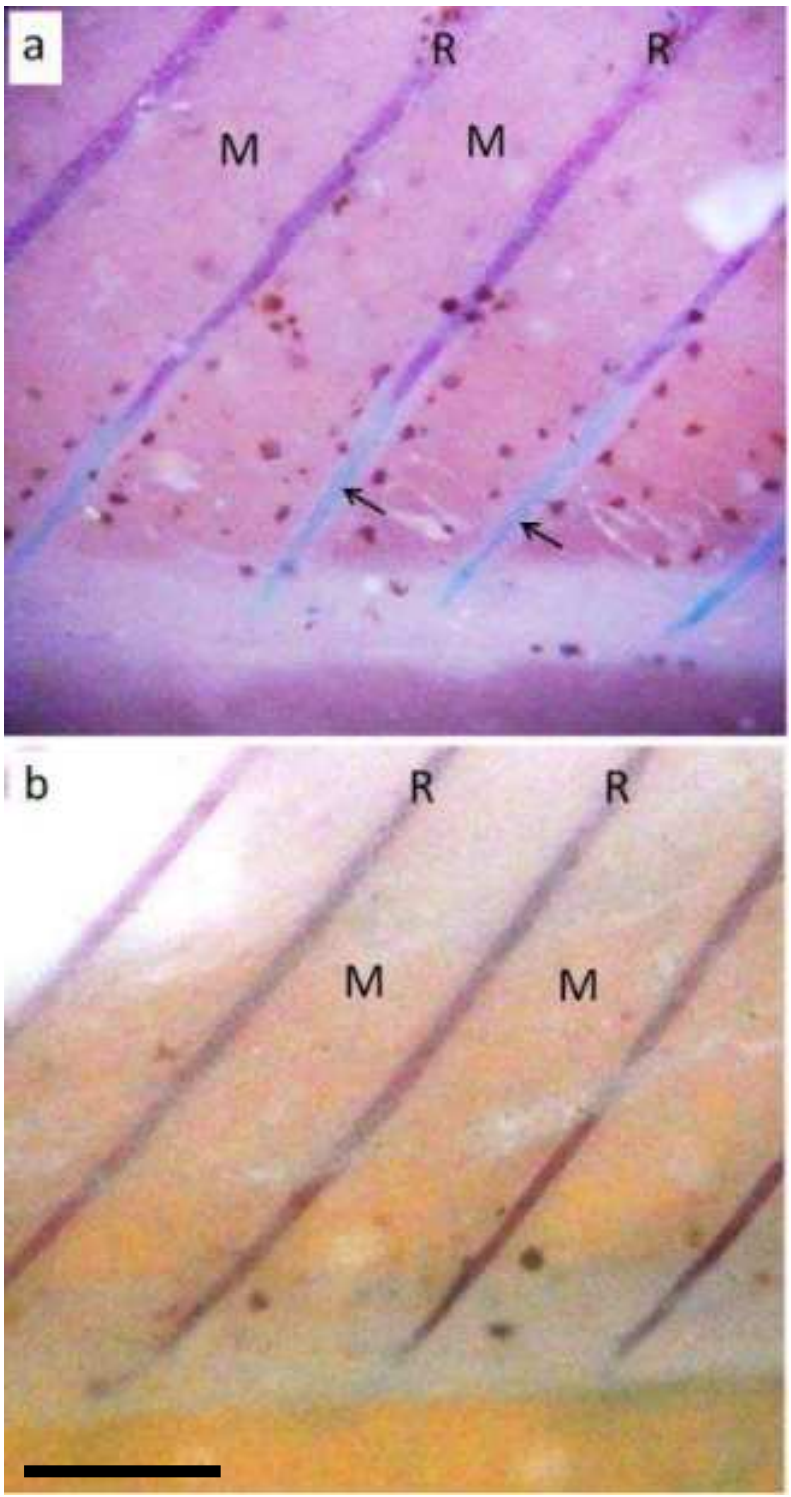

Figure 7.

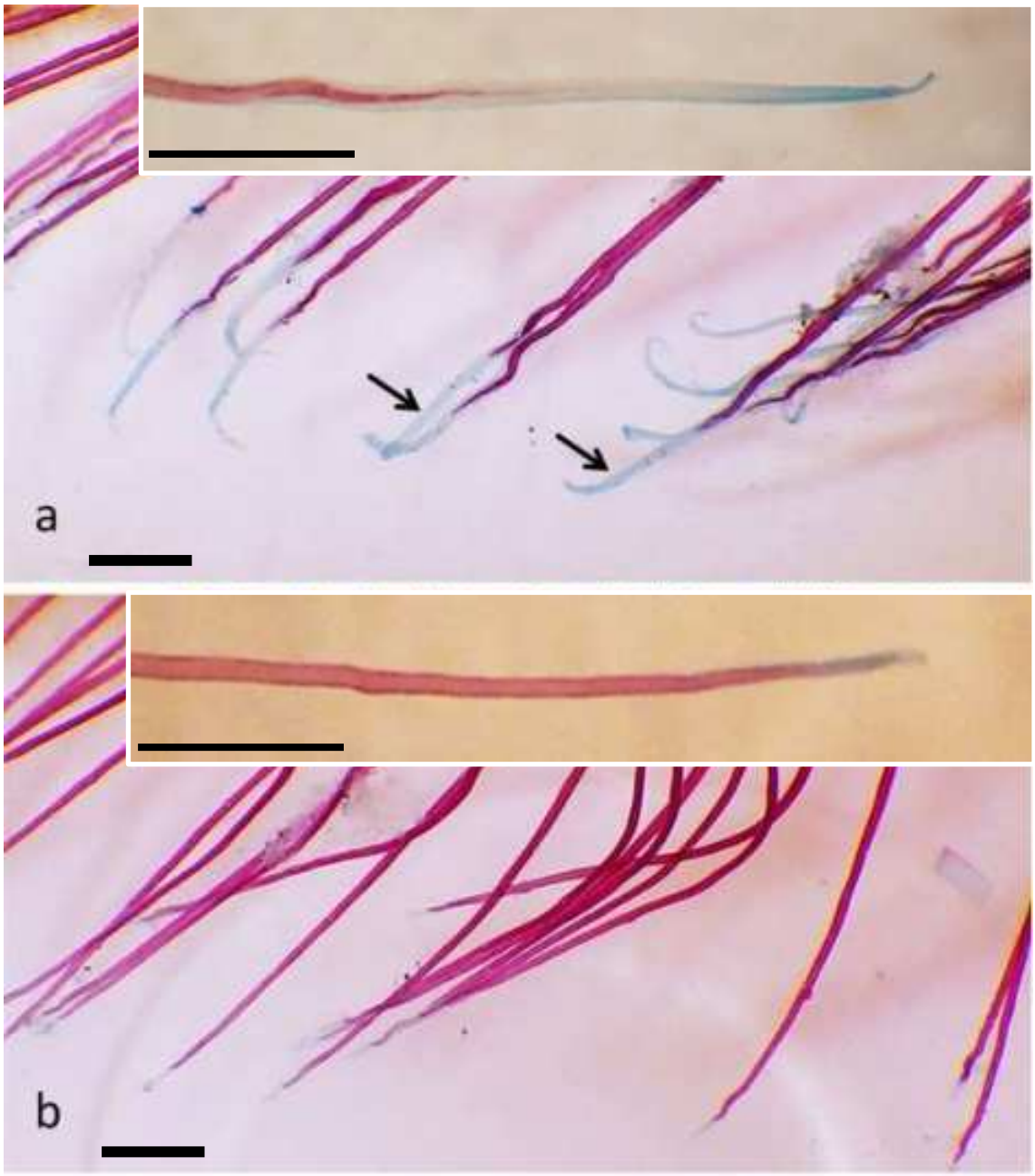

Figure 8.

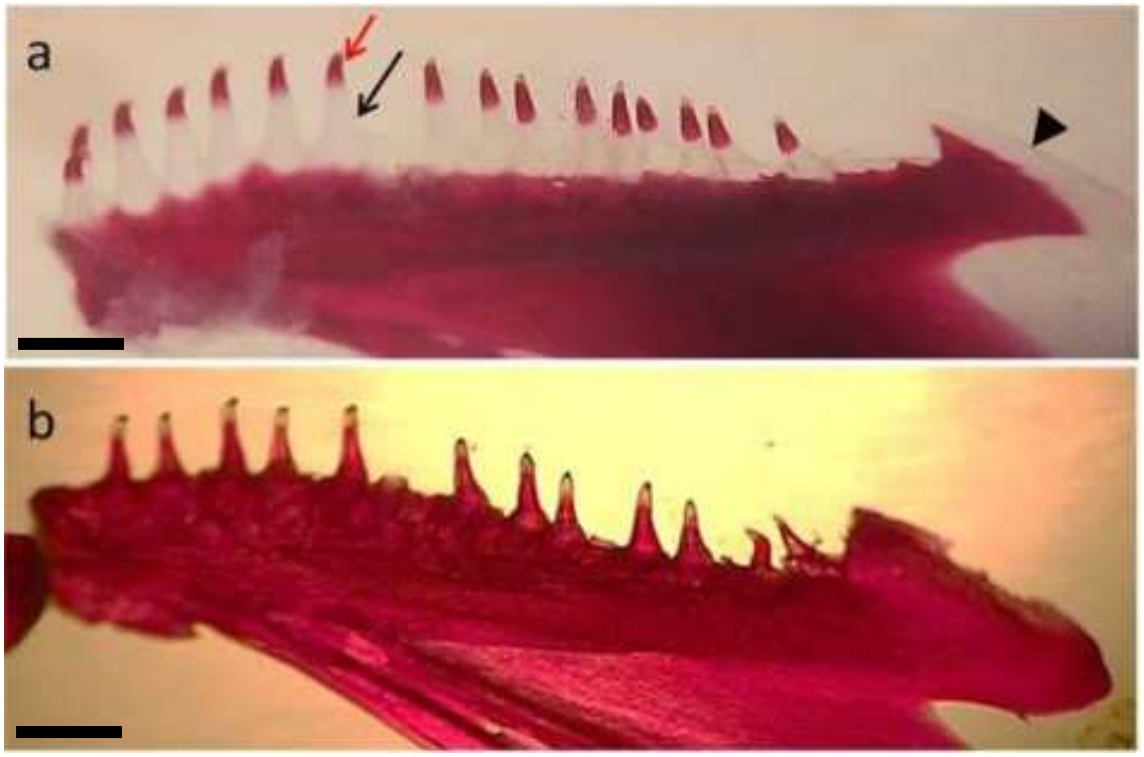

Figure 9.

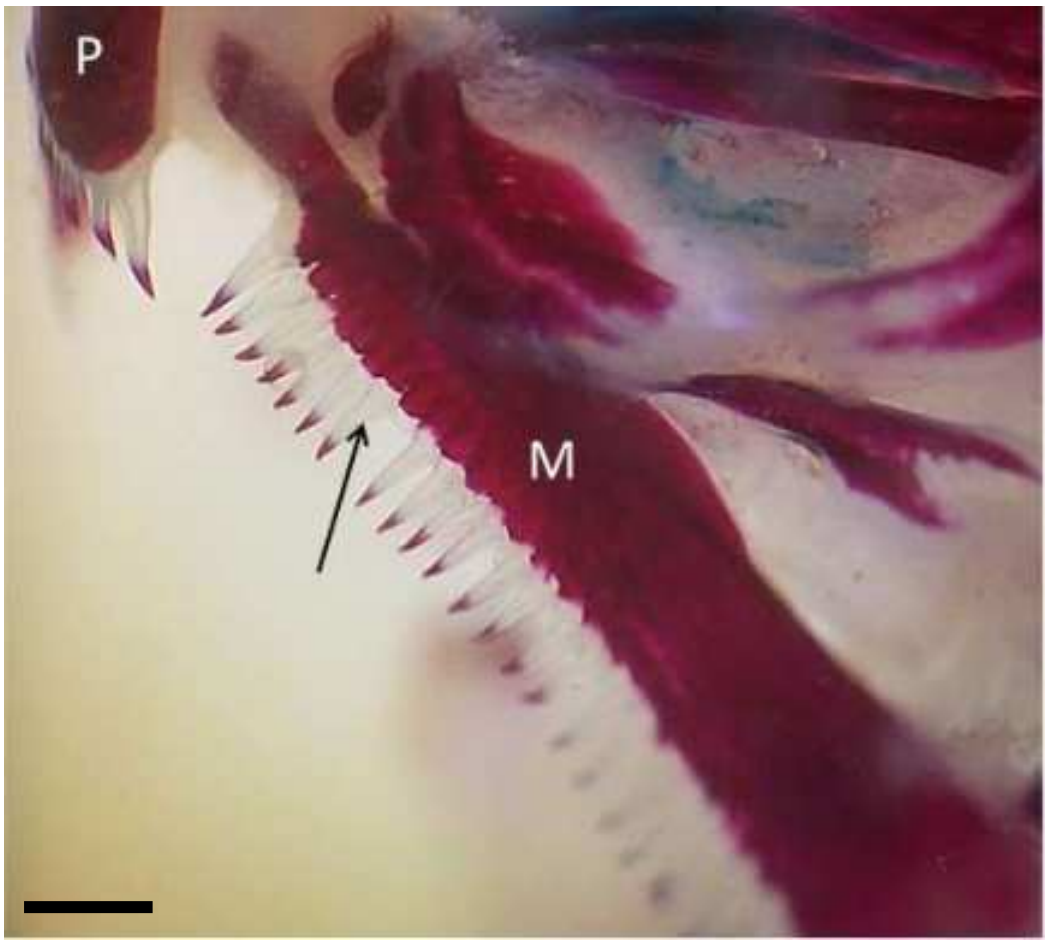

Figure 10.

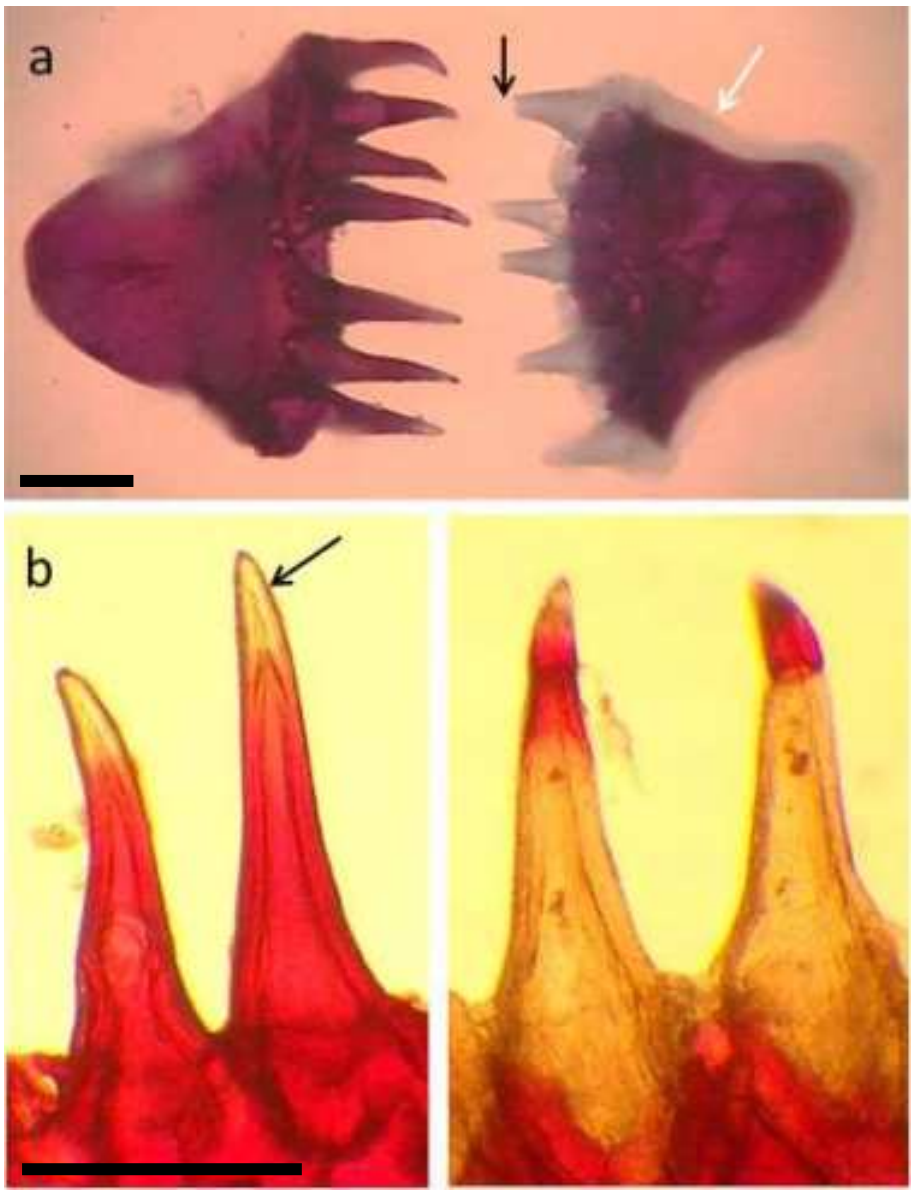

Figure 11.

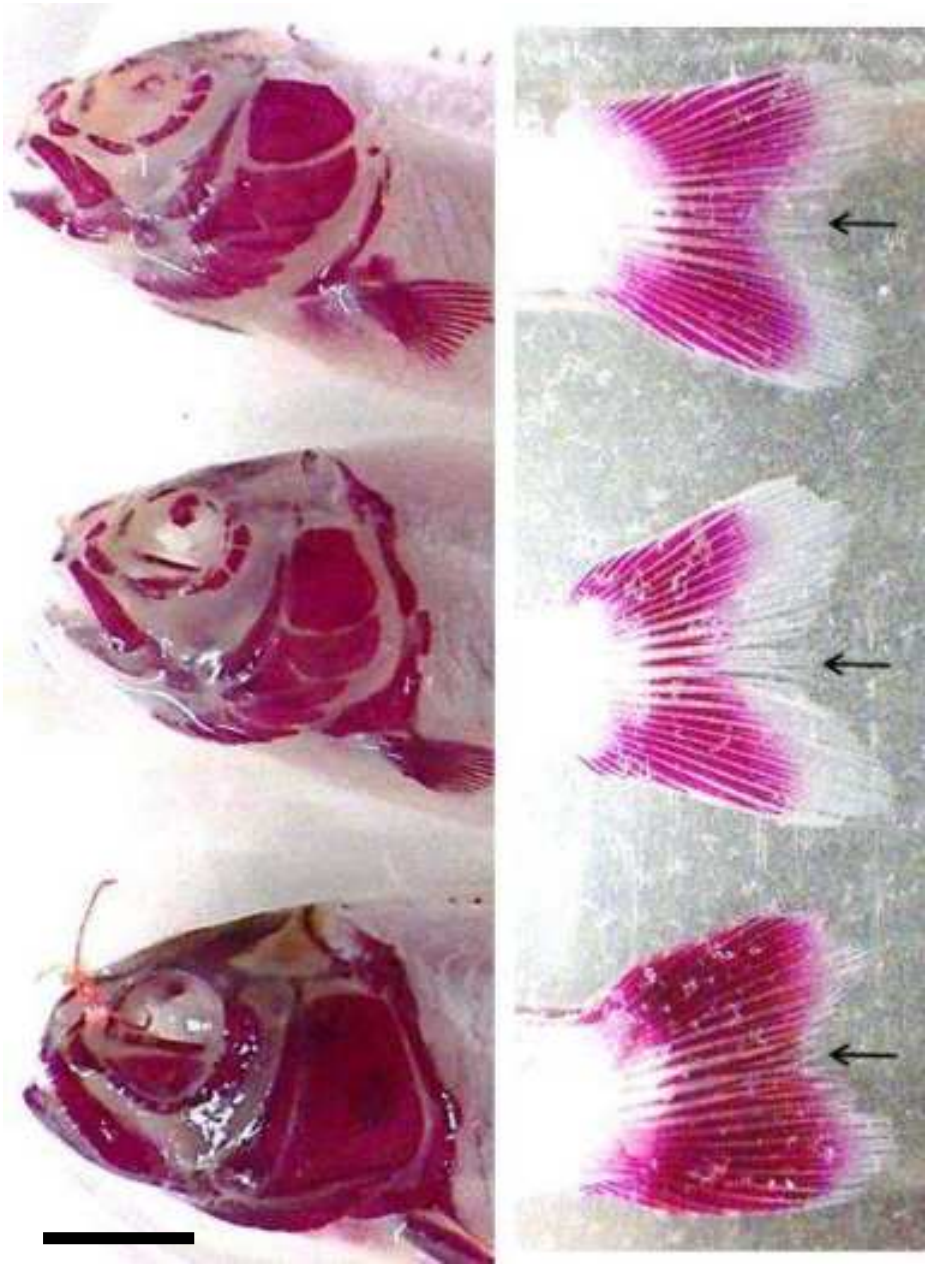

Figure 12.

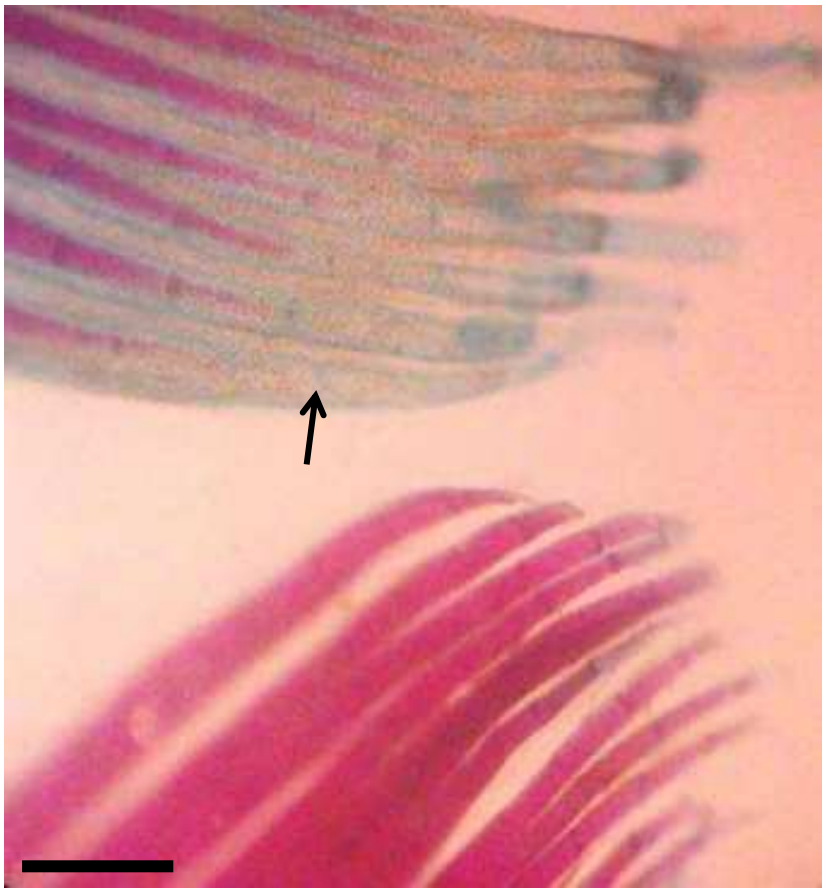

Figure 13.

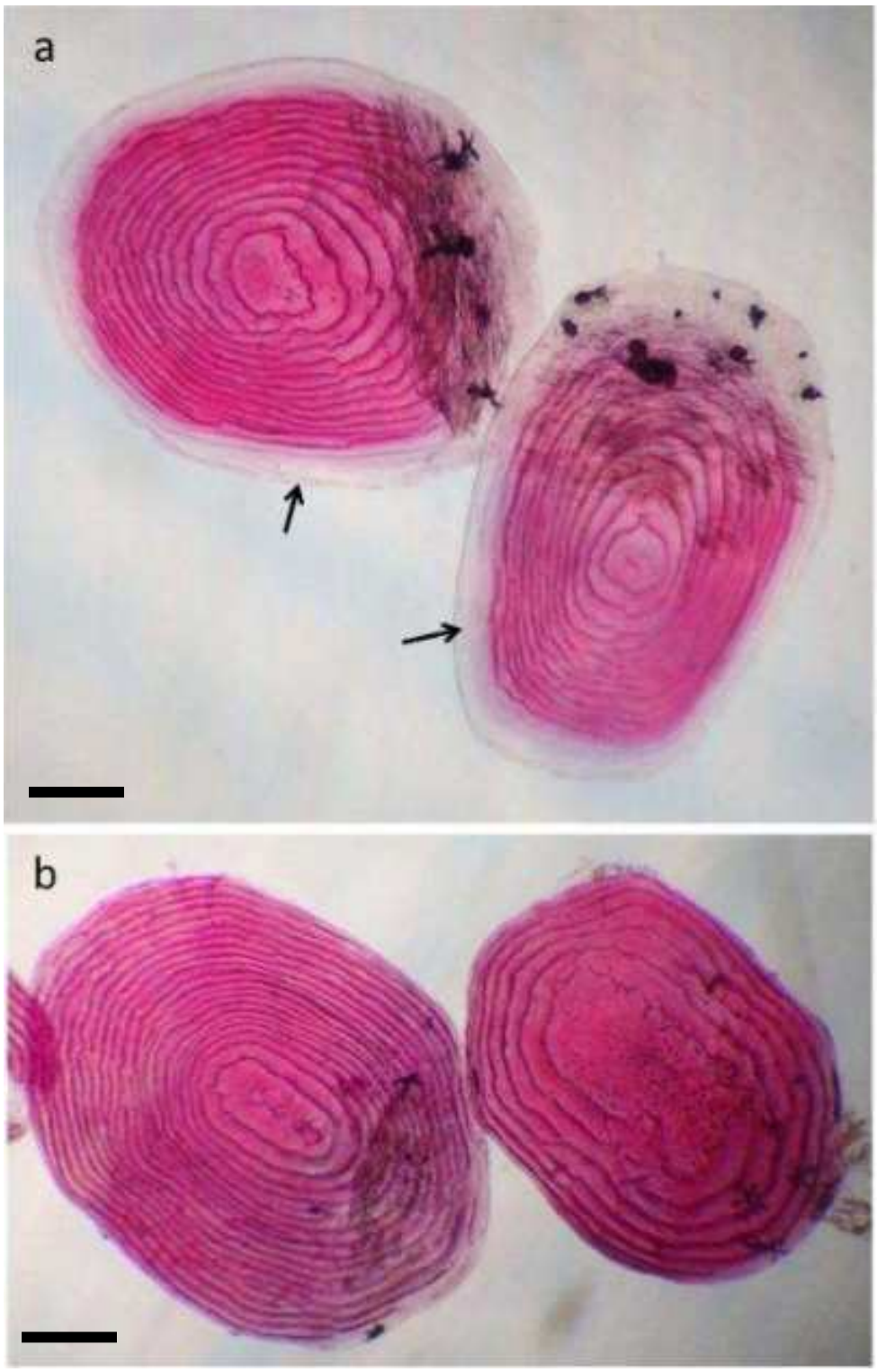

Figure 14.

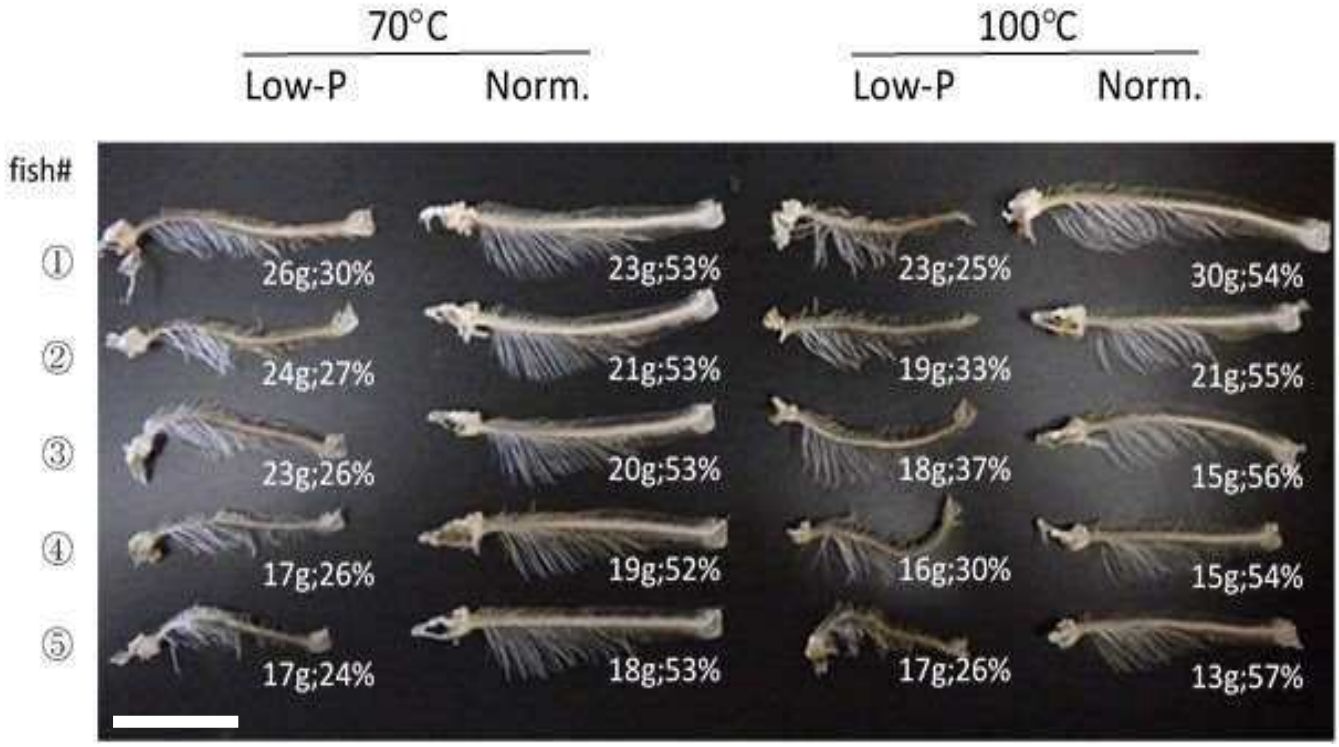
70°C
100°C
Low-P
Norm.
Low-P
Norm.
fish#
①
②
③
④
⑤
26g;30%
23g;53%
23g;25%
30g;54%
24g;27%
21g;53%
19g;33%
21g;55%
23g;26%
20g;53%
18g;37%
15g;56%
17g;26%
19g;52%
16g;30%
15g;54%
17g;24%
18g;53%
17g;26%
13g;57%

Figure 15.

Figure 16.

Figure 17.

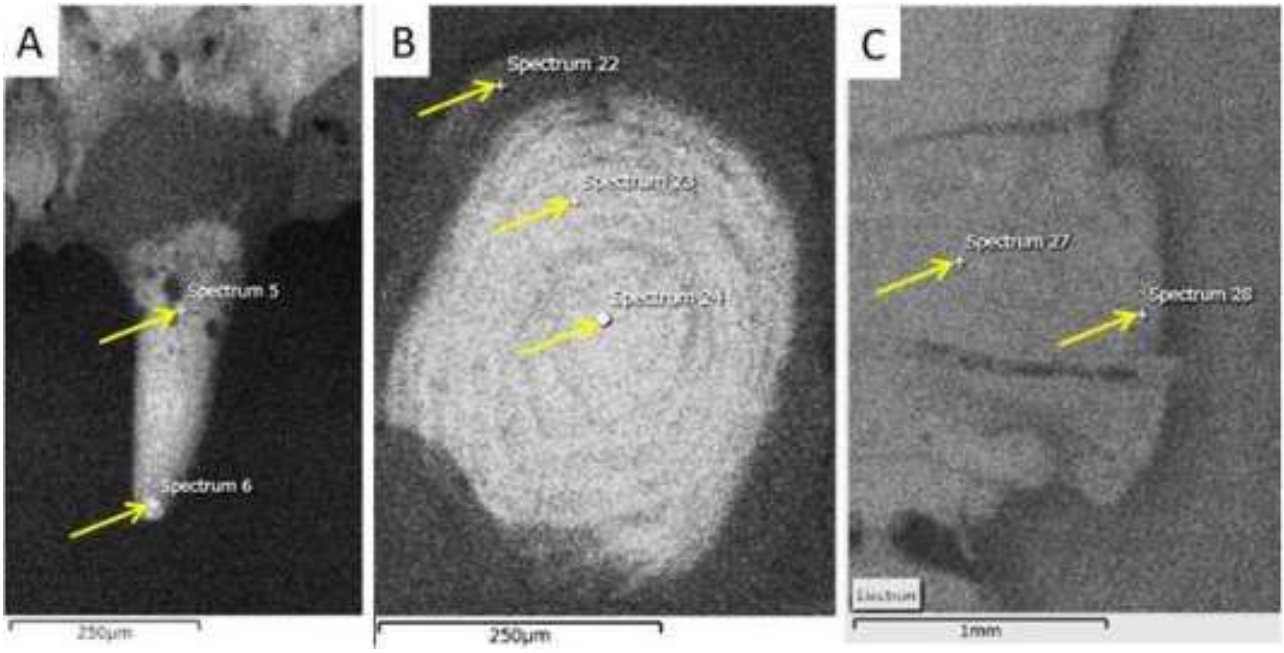
A
Spectrum 5
Spectrum 6
250µm
B
Spectrum 22
250µm
C
Spectrum 27
Spectrum 28
1mm

Figure 18.

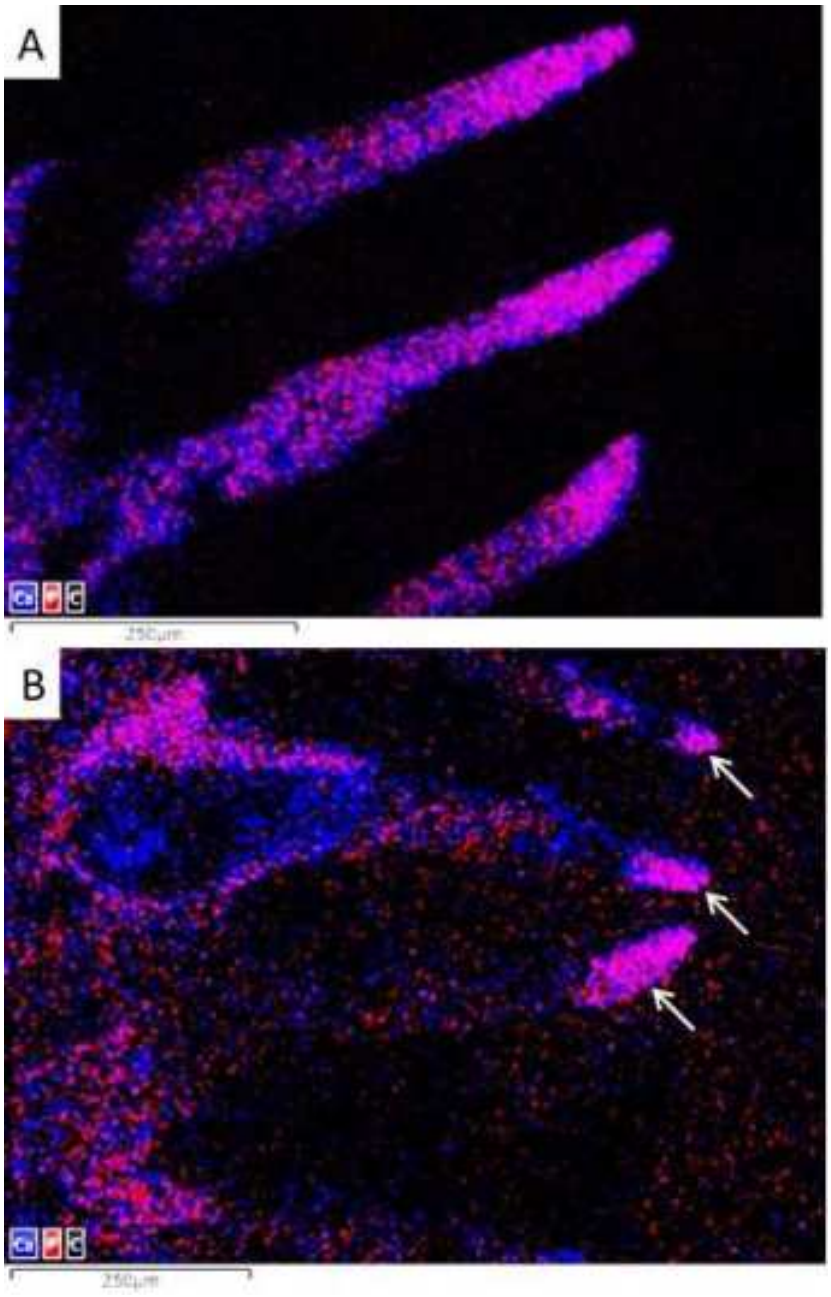

Figure 19.

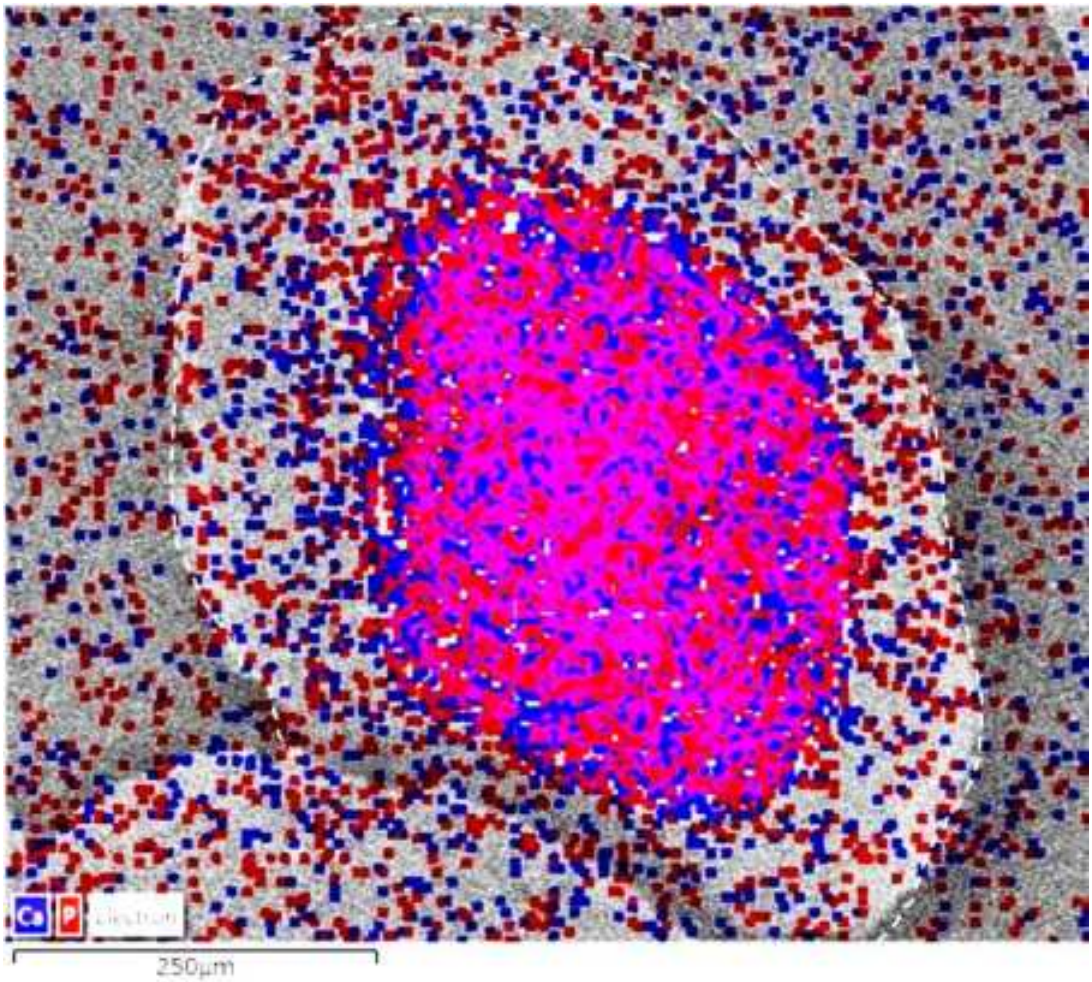

Figure 20.